ACS OMEGA

Open Access

http://pubs.acs.org/journal/acsodf

Article

Deciphering the miRNA−mRNA Interaction Landscape between Breast Cancer and Triple-Negative Breast Cancer: An Integrated Bioinformatics Approach

Ambritha Balasundaram, Tanisha Saurav Mitra, Iftikhar Aslam Tayubi, Hatem Zayed, and George Priya C. Doss*

Cite This: *ACS Omega* 2024, 9, 24379−24395

Read Online

ACCESS | Metrics & More | Article Recommendations | Supporting Information

ABSTRACT: Breast cancer (BC) is globally recognized as the second most prevalent form of cancer. It predominantly affects women and can be categorized into distinct types based on the overexpression of specific cancer receptors.The key receptors implicated in this context are the human epidermal growth factor receptor-2 (HER2), estrogen receptor (ER), and progesterone receptor (PR), alongside a particularly intricate subclass known as triple-negative breast cancer (TNBC). This subclassification is critical for the stratification of breast cancer and informs therapeutic decision-making processes. Due to a lack of therapeutic targets, such as growth factor receptors, TNBC is the most aggressive type. Hence, identifying targetable regulators such as miRNAs could pave the way for potential therapeutic interventions. To identify common differentially expressed mRNAs (DE-mRNAs) in BC, including TNBC, we leveraged two data sets from the GEO collection and The Cancer Genome Atlas (TCGA). Significant DE-mRNAs were identified through PPI, MCODE, CytoNCA, and CytoHubba analyses. Following this, miRNAs were predicted using mirDIP. We utilized GSE42568, GSE185645, and TCGA and identified 159 common DE-mRNAs. Using Cytoscape plug-ins, we identified the 10 most significant DE-mRNAs in BC. Using mirDIP, target miRNAs for 10 DE-mRNAs were identified. We conducted an advanced analysis on the TNBC GEO data set (GSE45498) to corroborate the significance of shared DE-mRNAs and DE-miRNAs in TNBC. We identified four downregulated DE-miRNAs, including hsa-miR-802, hsa-miR-1258, hsa-miR-548a-3p, and hsa-miR-2053, significantly associated with TNBC. Our study revealed significant miRNA−mRNA interactions, specifically hsa-miR-802/MELK, hsa-miR-1258/NCAPG, miR-548a-3p/CCNA2, and hsa-miR-2053/NUSAP1, in both BC and TNBC. The observed downregulation of hsa-miR-548a-3p is associated with diminished survival rates in BC patients, emphasizing their potential utility as prognostic indicators. Furthermore, the differential expression of mRNAs, including CCNB2, UBE2C, MELK, and KIF2C, correlates with reduced survival outcomes, signifying their critical role as potential targets for therapeutic intervention in both BC and TNBC. These findings highlight specific regulatory mechanisms that are potentially crucial for understanding and treating these cancer types.

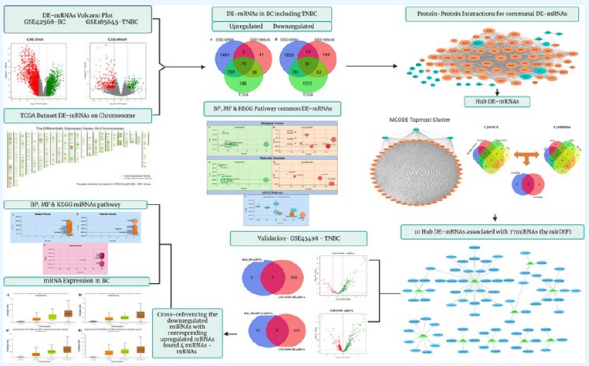

1. INTRODUCTION

Breast cancer (BC) is widely known as the most common cancer in women and ranks as the fifth leading cause of cancer-related deaths globally.[1] A significant observation involves BC prevalence and incidence variations across ethnic populations.[2] According to GLOBOCAN 2020 statistics, approximately 9.22 million new cancer cases were reported in females. BC constituted 2.26 million cases, roughly 24.5% female.[3] Invasive breast carcinoma (IBC) is a type of breast cancer that spreads into the surrounding breast tissue. Most types of breast cancer worldwide are found under the category of IBC, yet all types of invasive breast carcinoma are different. Two types of IBCs developed in humans are found most commonly among the population.[4] These include invasive ductal carcinoma and invasive lobular carcinoma. Other IBCs are found in minority populations like Medullary Carcinoma, Adenoid Cystic Carcinoma, Papillary Carcinoma, Medullary Carcinoma, Tubular Carcinoma, etc.[5]

BC can be classified into four subtypes: basal-like, luminal A, luminal B, and HER2-positive. These classifications are based on the presence of specific markers, such as ER, PR, and HER2.[6] Triple-negative breast cancer (TNBC), which is mostly included in the basal-like subclasses of BC. Approximately 15−20% of cancer cases among the four subtypes are

Received: January 1, 2024
Revised: April 13, 2024
Accepted: April 19, 2024
Published: May 29, 2024

represented by this category.[6,7] TNBC is included in the basal-like subtype of cancer due to its unique characteristics like the absence of ER/PR/HER2 receptors, risk of early relapse tendency, low survival rate, highly aggressive tumor growth, high recurrence potential, the huge chance of treatment rejections and highly invasive side effects, etc.[8,9] The aggressive characteristic of TNBC leads to its tendency to recur and metastasize to a higher level.[1] TNBC often occurs in young and premenopausal females.[7,10] TNBC lacks many treatments due to its variance compared to other kinds of breast cancer.[7] One of the most important reasons is the lack of therapeutic and curative targets. Because of the scarcity of biomarkers and therapeutic strategies, the only treatments available for TNBC are surgery, chemotherapy, and radiotherapy.[11] Two main types of chemotherapy effective for TNBC are neoadjuvant chemotherapy to shrink the tumor in size, followed by surgery and postoperative chemotherapy, which refers to continued chemotherapy.[12] The effectiveness of chemotherapy treatment is often contingent on the duration and consistency of the therapy; delays or extended treatment periods can potentially diminish its effectiveness. One particular concern with TNBC is its propensity to metastasize in the brain, resulting in a high risk of recurrence.[7,12] It is also been claimed that around 30% of metastatic TNBC would survive at least 5 years after initial diagnosis under the condition of undergoing systematic chemotherapy treatment. It has also been virtually determined that all metastatic TNBC patients will eventually die.[8,13]

Scientists use Microarray analysis and RNA sequencing to identify biomarkers and targets that can help stabilize the abnormalities caused by invasive breast carcinoma.[7,9] The epigenetic alterations and miRNA dysregulation can silence gene expression, especially in TNBC, and activate/suppress the multiple numbers of genes at pre- and post-transcriptional stages.[9] miRNAs are small, noncoding RNA and endogenous sequences of approximately 19−25 base pairs. miRNAs also affect the negative regulation and inhibition of specific mRNA targets' gene expression.[14] Hence, comprehending the processes and signaling pathways governed by mRNAs and their linked miRNAs could be beneficial for diagnosing and treating cancers.

We analyzed the gene expression patterns of BC and TNBC tissues using GEO data sets and breast cancer (BRCA) samples from the TCGA database compared to normal samples. We have identified biomarkers that can contribute to a more efficient and personalized treatment approach for BC, including TNBC. This treatment approach was achieved by pinpointing common DE-mRNAs and their associated DE-miRNAs across these data sets. Furthermore, these findings suggest a connection between miRNA−mRNA networks implicated in BC's development, including TNBC.

2. MATERIALS AND METHODS

2.1. Data Collection and Identification of DE-mRNAs. We retrieved the GEO data sets in the NCBI database using the following keywords "Breast Cancer", "TNBC (or) triple-negative breast cancer", and "*Homo sapiens*". The data set underwent filtering based on the following criteria: (i) It should include a higher number of BC or TNBC samples; (ii) availability of raw data in the GEO data sets; and (iii) data sets with normal or control samples.[15] Based on these criteria, we obtained the GSE42568 GEO Data Set containing breast cancer and normal tissues from the NCBI database. The GSE42568 data set comprised 104 breast cancer samples. From this, 82 were invasive ductal carcinoma, 17 were invasive lobular, five belonged to special type (two were tubular and three were mucinous), and 17 were normal. Among these were 67 (+) and 34 ER (−) samples. Similarly, we obtained the GSE185645 GEO data set containing TNBC and normal samples. We utilized the GEO2R tool to screen the differently expressed mRNAs (DE-mRNAs) in BC with ER+/ER− and TNBC data sets. DE-mRNAs with $|\log2FC| \geq 1$ and *a* *p*-value ≤ 0.05 were regarded as significantly upregulated, while those with $|\log2FC| \leq -1$ and *p*-values ≤ 0.05 were deemed significantly downregulated. The significant up- and down-regulated DE-mRNAs in breast cancer and TNBC were visualized in the volcano plot. Following that, we utilized the BRCA samples in the TCGA database and obtained DE-mRNAs with *a* cutoff of $|\log2FC| +1 \geq$ or ≤ -1 and *p*-values ≤ 0.05 using the Gene Expression Profiling Interactive Analysis 2 (GEPIA2) portal.[16] The significant DE-mRNAs in BRCA were visualized in the chromosome. We obtained the common DE-mRNAs among BC with ER+/ER−, TNBC, and TCGA-BRCA samples using the Venn diagram compared to normal or control samples. Venn diagrams were constructed using the "Bioinformatics & Evolutionary Genomics" software tool hosted by VIB-UGENT Centre for Plant System Biology, VIB, and GHENT University.

2.2. Functional Annotation and Enrichment Analysis. Gene ontology (GO) analysis is applied to communal DE-mRNAs from BC, including TNBC, in the DAVID online web server.[17] The GO classification of biological process (BP), molecular function (MF), and KEGG Annotation were examined. The DE-mRNA's significant GO biological process, GO Molecular Functions, and KEGG Pathways were visualized in bubble plots using a *p*-value cutoff of <0.05.

2.3. Protein−Protein Interactions (PPI) Network Construction. We utilized the STRING tool, an online database, to build a PPI network to analyze the relationships between the significant upregulated and downregulated communal DE-mRNAs.[18] The confidence during the PPI network was set to 0.7 (high confidence value). Once the PPI network was built, we removed all of the disconnected and free nodes that do not branch to the main PPI network cluster. Then, the output PPI network was downloaded and examined using Cytoscape software.[19] We applied the Cytoscape network analyzer app to visualize the PPI network better. Cytoscape is used to visualize and explore the interactions between the significant DE-mRNAs.

2.4. Identification of Hub DE-mRNAs Using MCODE, CytoNCA, and CytoHubba Analysis. For further specificity in the investigation, MCODE analysis was performed on a Cytoscape network analyzer tool. The topmost cluster from the PPI network was picked from the MCODE analysis. This chosen cluster was further processed using CytoNCA and CytoHubba plug-ins to detect the hub DE-mRNAs. The cytoNCA analysis of the module 1 network was analyzed using four parameters, namely, EPC, MCC, MNC, and Stress. The top 20 DE-mRNAs in each CytoNCA parameter were selected.

On the other hand, the CytoHubba analysis was performed using four parameters, namely, Betweenness, Closeness, eigenvector, and LAC. Similarly, the top 20 DE-mRNAs in each CytoHubba parameter were selected. The DE-mRNAs in each parameter were observed and recorded for further utilization. Lastly, these recorded DE-mRNA outputs from each parameter were used to construct a Venn Diagram to identify the hub DE-mRNAs by the presence of shared DE-

https://doi.org/10.1021/acsomega.4c00011
ACS Omega 2024, 9, 24379−24395

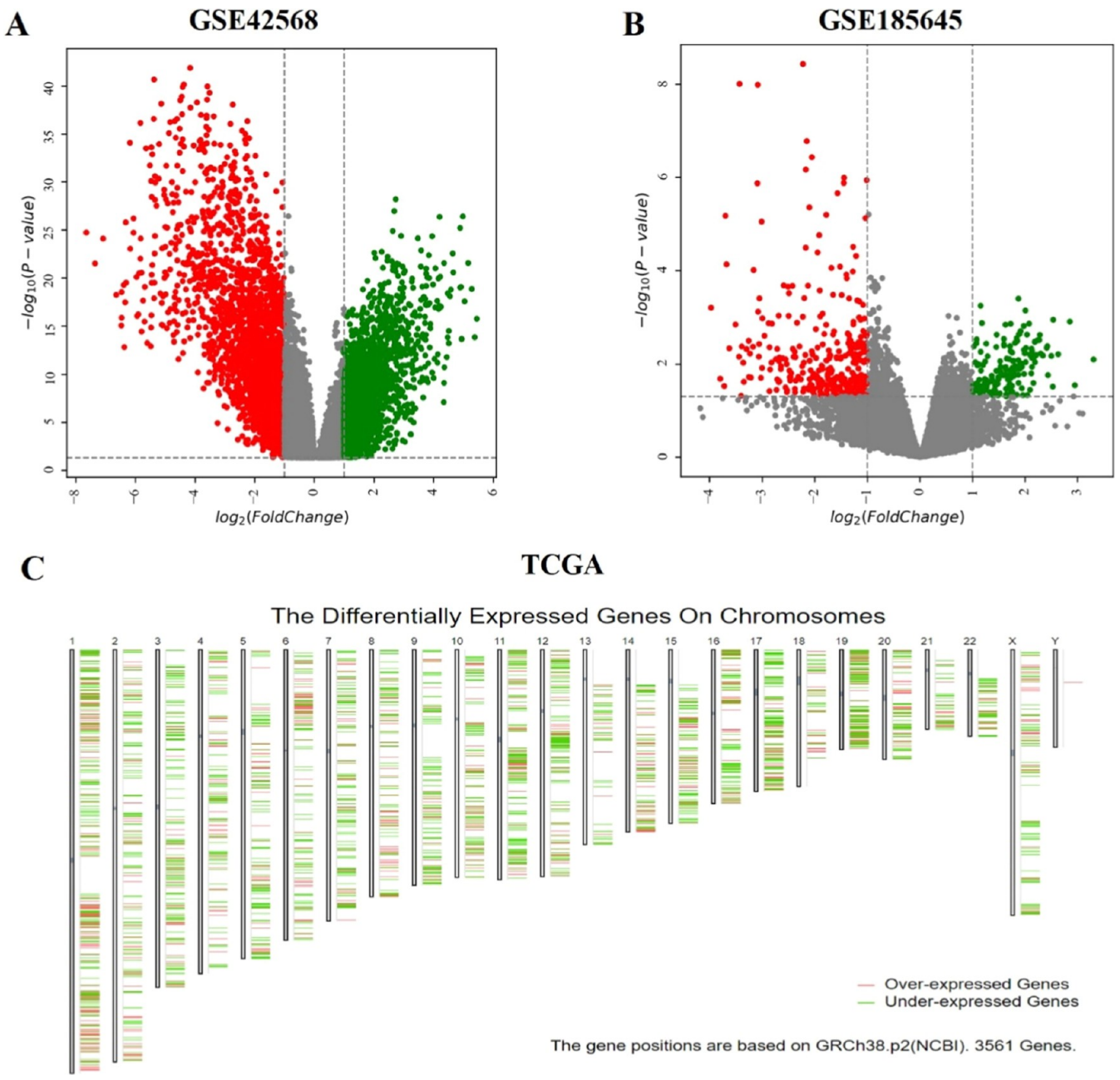

Figure 1. Identification of DE-mRNAs in GSE42568, GSE185645, and TCGA data sets. (A) Volcano plot of GSE42568 representing the comparison of gene expression between BC and normal. (B) Volcano plot of GSE185645 representing the comparison of gene expression between TNBC and normal. The red dot indicates downregulated DE-mRNAs (logFC ≥ -1; $p \leq 0.05$), while the green dot indicates upregulated DE-mRNAs (logFC $\geq +1$; $p \leq 0.05$). (C) DE-mRNAs on chromosomes representing the comparison of gene expression between BRCA and normal samples from the TCGA data set. The red band indicates upregulated DE-mRNAs (logFC $\geq +1$; $p \leq 0.05$), while the green band indicates downregulated DE-mRNAs (logFC ≥ -1; $p \leq 0.05$).

mRNAs across the parameters of cytoNCA and cytoHubba analysis using "Bioinformatics & Evolutionary Genomics" software tool hosted by VIB-UGENT center for plant system biology, VIB and GHENT University.

2.5. Validation of hub DE-mRNAs in BC. To assess the expression levels of the pivotal hub DE-mRNAs in tissues and conduct survival analysis, GEPIA2 (http://gepia2.cancer-pku.cn/)[16] and OncoLnc (http://www.oncolnc.org/) were used. These two online platforms facilitate the analysis and exploration of data sets derived from TCGA. Utilizing this resource, we scrutinized the expression profiles of key hub DE-mRNAs within BRCA tissues using GEPIA2. Furthermore, we assessed these hub DE-mRNAs' overall survival (OS) correlations in breast cancer patients using the Kaplan–Meier plot of OncoLnc. The median cutoff segregates patients into two categories: those with mRNA expression levels above the 50th percentile, termed the high expression group, and those below the 50th percentile, termed the low expression group. Statistical significance was determined with a threshold of p-value ≤ 0.05.

2.6. Prediction of Hub DE-mRNAs-Associated miRNAs. The hub DE-mRNAs were uploaded into mirDIP to identify miRNAs that target these uploaded mRNAs.[20] The minimum score class to identify the associated miRNAs was

https://doi.org/10.1021/acsomega.4c00011
ACS Omega 2024, 9, 24379−24395

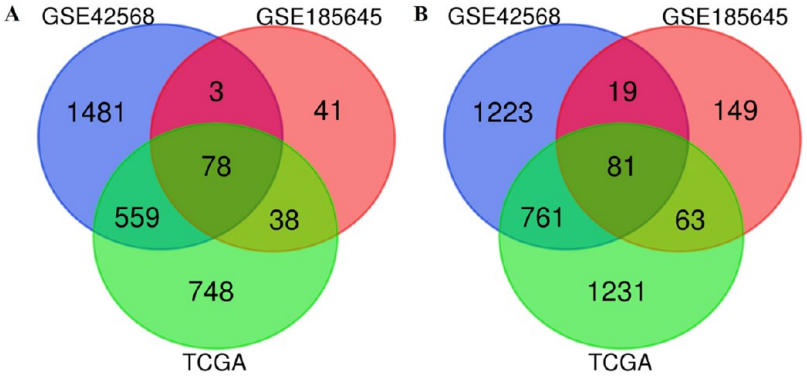

Figure 2. Overlap DE-mRNAs between the data sets. (A) Venn diagram of the 78 communal upregulated DE-mRNAs between BC, including TNBC and normal. (B) Venn diagram of the 81 communally downregulated DE-mRNAs in BC and TNBC.

set to a very high class (Top 1%) in the mirDIP web server. The resulting hub DE-mRNAs associated miRNAs network for BC was visualized with Cytoscape Software.

The obtained DE-mRNAs and their associated miRNAs were further validated using the TNBC GEO Data set. The GEO Data set GSE45498 consists of miRNA and mRNA profiling of the TNBC patient tumor samples against adjacent normal samples. In GSE45498, miRNAs and mRNAs profiling were generated from the GPL16231 and the GPL16299 platform, respectively. Significant DE-miRNAs and DE-mRNAs were identified in TNBC patients by using the GEO2R tool. Finally, to validate the hub DE-mRNAs and their associated miRNAs, the significant DE-miRNAs from GSE45498 overlapped with hub DE-mRNA-associated miRNAs. Similarly, the significant DE-mRNAs from GSE45498 overlapped with the hub DE-mRNA. The resulting hub DE-mRNA and DE-miRNA can be utilized as BC and TNBC biomarkers.

2.7. Validation of Hub DE-mRNA/DE-miRNAs. The University of Alabama Cancer (UALCAN) is a comprehensive, easily operatable, interactive online platform (http://ualcan.path.uab.edu) for thoroughly evaluating the TCGA gene expression data. It enabled us to examine the relative expression of a core DE-mRNA in tumor and normal tissues and in different tumor subclasses depending on distinct Breast cancer stages. The expression of the core DE-mRNA was validated via UALCAN for BRCA related to its subclasses and normal using TCGA and GTEx data sets.[21]

We conducted a rigorous validation of DE-mRNAs' translational profiles using the Human Protein Atlas (HPA) database (https://www.proteinatlas.org/). Specifically, we utilized immunohistochemistry (IHC) pathological sections from both normal and BC samples to corroborate our results. The translation levels of the key hub DE-mRNAs were assessed by examining the HPA database, which offers comprehensive information about human protein distribution in various tissues and cells. The database annotates protein expression in tissues based on Intensity and Quantity. Similarly, we validated the expression levels of the crucial hub DE-miRNAs in TCGA-BRCA, along with survival analysis, using the OncoLnc database. In this cutoff analysis, patients were categorized into two groups: those in the bottom and the top quartile.

2.8. Functional Enrichment Analysis of DE-miRNAs. Functional enrichment analysis for hub DE-miRNAs of BC, including TNBC, was performed by using DIANA tools. DIANA-miRPath v.3 is an online toolkit for evaluating miRNA regulatory functions and locating regulated pathways, GO biological processes, and molecular functions.[22] The BP, MF, and KEGG pathway analysis for DE-miRNAs was carried out, and the significant functions and pathways were identified with $p < 0.05$.

3. RESULTS

3.1. Identification of Differently Expressed mRNA (DE-mRNAs). The GSE42568 data set comprises the gene expression patterns of 104 patient's tumor samples with breast cancer, and 17 normal samples were retrieved from the GEO database. The GSE42568 data set was produced from the GPL570 platform. Similarly, the GSE185645 data set includes the gene expression patterns of 15 patient tumor samples with TNBC retrieved from the GEO database. The GSE185645 data set was generated from the GPL6244 platform. We determined the DE-mRNAs between breast cancer (BC with ER+/ER− & TNBC) patients and normal controls using the GEO2R tool. The DE-mRNAs were identified with the cutoff values of $|\log2FC| + 1 \geq$ (upregulated DE-mRNAs) and $|\log2FC| \leq -1$ (downregulated DE-mRNAs) with p-values ≤ 0.05, obtained using the built-in R/Bioconductor limma package from the GEO2R web server tool. The significant DE-mRNAs of GSE42568 and GSE185645 data sets with the above-matched criteria were identified and represented in volcano plots, where the green dots signify upregulated mRNAs and the red dots signify downregulated mRNAs (Figure 1A,B). The TCGA data contains 1085 patient tumor samples of BRCA and 112 normal samples along with GTEx 179 normal samples were deposited on the GEPIA2 Web site, which was utilized in differential expression analysis function with the limma differential method to identify the BRCA patients DE-mRNAs. Using the GEPIA2 Web site, we discovered that DE-mRNAs of BRCA were represented on the chromosomes (Figure 1C).

Following the differential expression analysis, we identified 4205 DE-mRNAs (2121 upregulated and 2084 downregulated) in the GSE42568 and 427 DE-mRNAs (160 upregulated and 312 downregulated) in the GSE185645 as well as 3559 DE-mRNAs (1423 upregulated and 2136 downregulated) in the TCGA data set. After overlapping the DE-mRNAs of 2 GEO data sets with the TCGA data set, 159 DE-mRNAs (78 upregulated and 81 downregulated) were obtained and visualized in the Venn diagram (Figure 2).

https://doi.org/10.1021/acsomega.4c00011
ACS Omega 2024, 9, 24379−24395

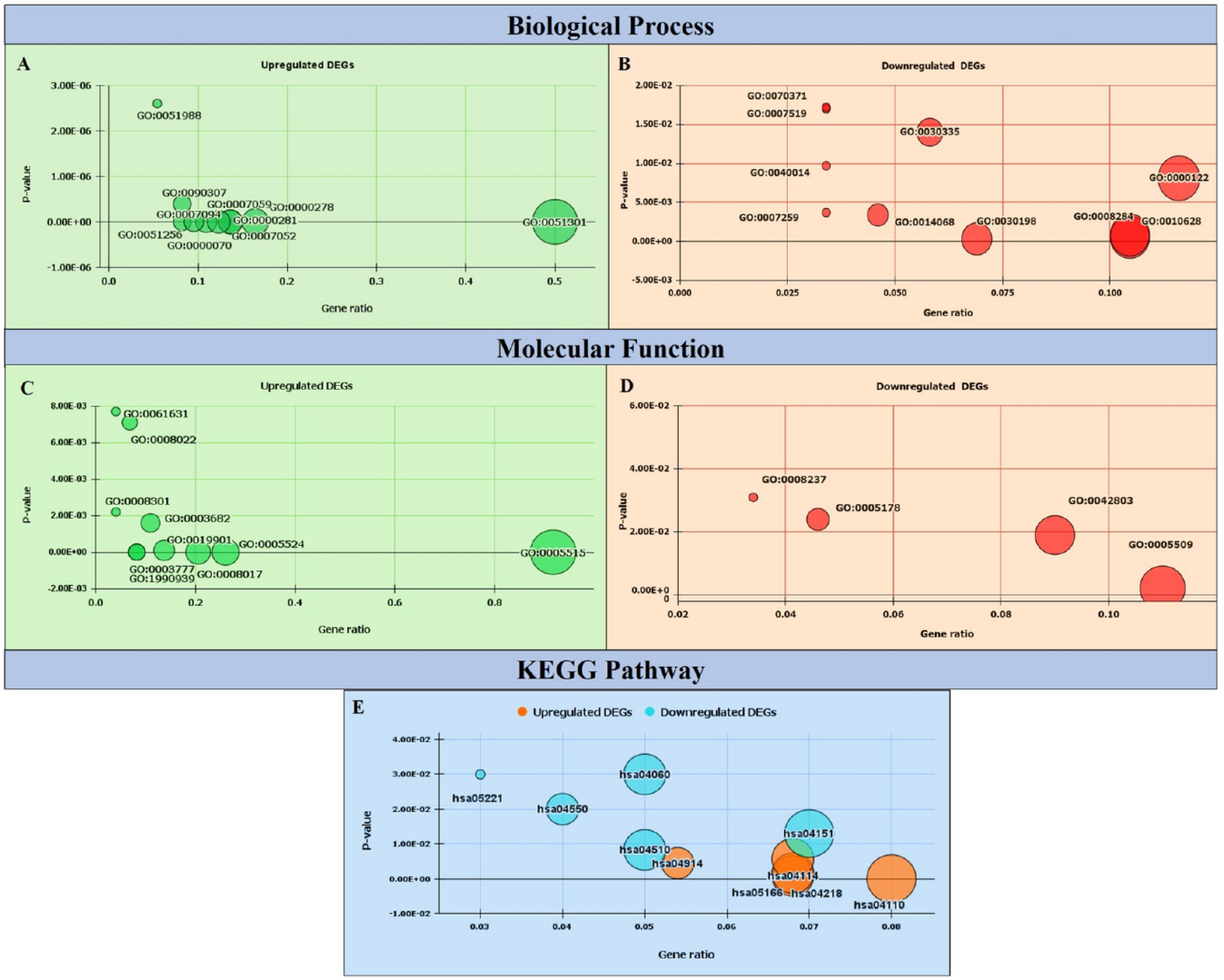

Figure 3. Bubble plot of the GO biological process, GO molecular functions, and KEGG pathway analysis of DE-mRNAs. A bubble indicates a GO term, with the size of the bubble representing the number of genes in the GO term. The *X*-axis represents the gene ratio, and the *Y*-axis represents the p-value. (A) The significantly enriched biological process of upregulated DE-mRNAs, (B) the significantly enriched biological process of downregulated DE-mRNAs, (C) the significantly enriched molecular functions of upregulated DE-mRNAs, (D) the significantly enriched molecular functions of downregulated DE-mRNAs, and (E) the significantly enriched KEGG pathways of upregulated and downregulated DE-mRNAs.

3.2. Enrichment Analysis. The GO analysis was applied to all 159 DE-mRNAs from BC, including TNBC, to identify their significant functions via the DAVID online web server. The most significant GO BP, MF, and KEGG pathways of BC DE-mRNAs were visualized in the bubble plots (Figure 3). The GO classification of BP, MF, and KEGG annotation was considered significant with $p < 0.05$.

We revealed that the biological process of upregulated DE-mRNAs was enriched in cell division (GO:0051301), mitotic cytokinesis (GO:0000281), mitotic spindle organization (GO:0007052), mitotic sister chromosome segregation (GO:0000070), mitosis (GO:0000278), mitotic spindle midzone assembly (GO:0051256), chromosome segregation (GO:0007059), mitotic spindle assembly checkpoint signaling (GO:0007094), mitotic spindle assembly (GO:0090307), and regulation of attachment of spindle microtubules to the kinetochore (GO:0051988) (Figure 3A). The biological process of downregulated DE-mRNAs was enriched in positive regulation of gene expression (GO:0010628), extracellular matrix organization and biogenesis (GO:0030198), positive regulation of cell population proliferation (GO:0008284), positive regulation of PI3Ksignaling (GO:0014068), regulation of multicellular organism growth (GO:0040014), inhibition of transcription from RNA polymerase II promoter (GO:0000122), receptor signaling pathway via JAK-STAT (GO:0007259), positive regulation of cell migration (GO:0030335), skeletal muscle tissue development (GO:0007519), and ERK1 and ERK2 cascades (GO:0070371) (Figure 3B).

The significant MFs that corresponded to upregulated DE-mRNAs were protein binding (GO:0005515), microtubule motor activity (GO:0003777), microtubule motor activity (GO:0003777), protein kinase binding (GO:0019901), chromatin binding (GO:0003682), ubiquitin-conjugating enzyme activity (GO:0061631), DNA bending involving DNA binding (GO:0008301), ATP binding (GO:0005524), and obsolete protein C-terminal binding (GO:0008022) (Figure 3C). In contrast, the most significant molecular

https://doi.org/10.1021/acsomega.4c00011
ACS Omega 2024, 9, 24379−24395

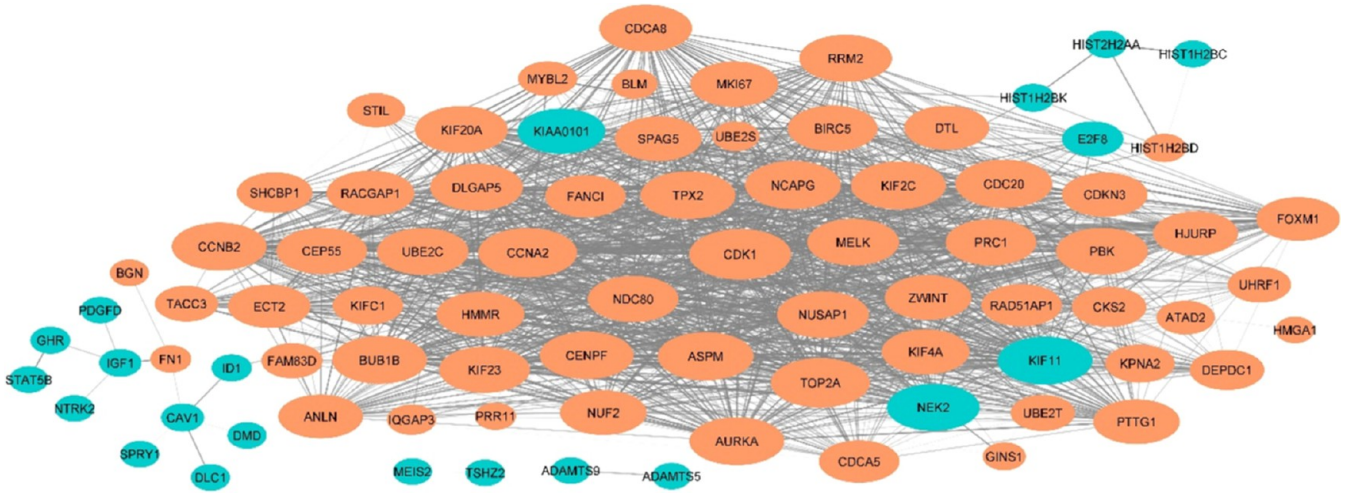

Figure 4. Protein−protein interaction network of the up- and downregulated DE-mRNAs. Spheres and lines indicate nodes and edges, respectively. Spheres represent proteins, and their molecular interactions are represented by lines. The larger sphere represents higher degrees, and the thicker line represents the higher combined scores. Orange nodes indicate the upregulated DE-mRNAs, and blue nodes indicate the downregulated DE-mRNAs.

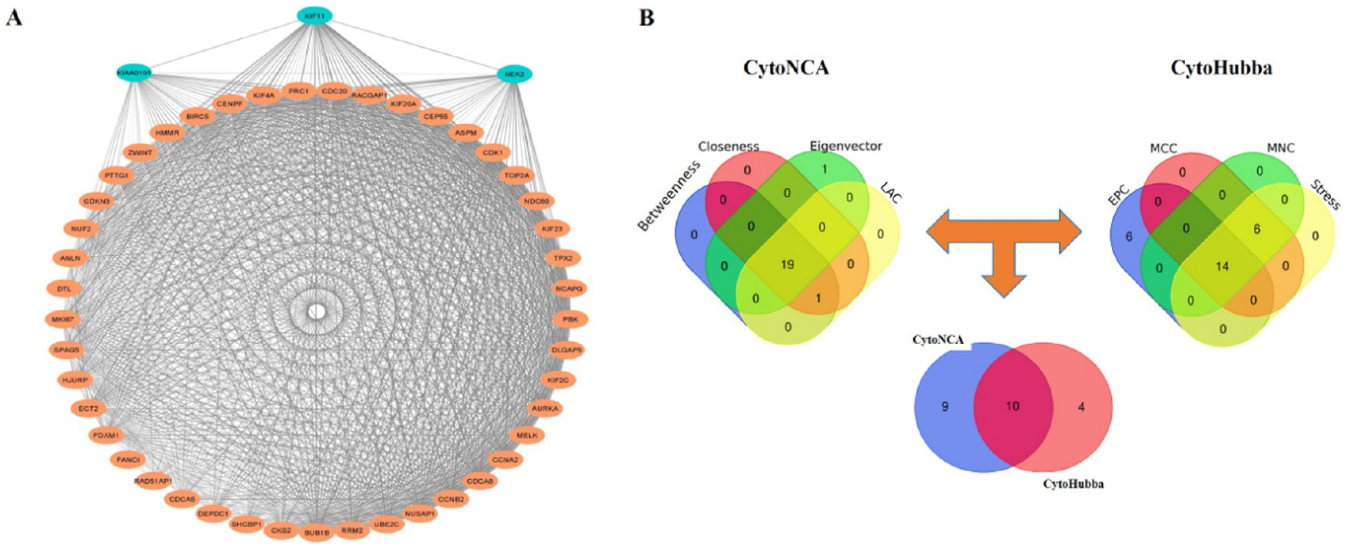

Figure 5. (A) Topmost significant module (Module 1) of DE-mRNAs from the PPI network. (B) The Venn diagram on the right-hand side showed 19 overlapped DE-mRNAs from the top 20 DE-mRNAs of four distinct CytoNCA algorithms: Betweenness, Closeness, eigenvector, and LAC. The Venn diagram on the left-hand side showed 14 overlapped DE-mRNAs from the top 20 DE-mRNAs of the four distinct CytoHubba algorithms: EPC, MCC, MNC, and Stress. The Venn diagram in the middle showed 10 overlapped DE-mRNAs between CytoNCA and CytoHubba.

functions that corresponded to downregulated DE-mRNAs were calcium ion binding/storage activity (GO:0005509), integrin binding (GO:0005178), protein homodimerization activity (GO:0042803), metallopeptidase activity (GO:0008237), muscle α-actinin binding (GO:0051371), NOS binding (GO:0050998), protein-macromolecule adaptor activity (GO:0030674), metalloendopeptidase activity (GO:0004222), PKA binding (GO:0051018), and extracellular matrix structural constituent (GO:0005201) (Figure 3D).

Furthermore, the KEGG pathway analysis exposed the involvement of upregulated DE-mRNAs in the Oocyte meiosis (hsa04114), cell cycle (hsa04110), and Cellular senescence (hsa04218), whereas downregulated DE-mRNAs were involved in the PI3K-Akt signaling pathway (hsa04151), focal adhesion (hsa04510), Signaling pathways regulating pluripotency of stem cells (hsa04550), Acute myeloid leukemia (hsa05221), and Cytokine-cytokine receptor interaction (hsa04060) (Figure 3E).

3.3. Establishment of PPI Network. We utilized the STRING to establish the physical and functional relationships between the DE-mRNAs in BC. A high confidence level of 0.70 was set as the minimal interaction score, and unconnected nodes were removed. The obtained network from STRING was further visualized by using Cytoscape software. The established PPI network has 84 nodes and 1379 edges, where nodes stand for DE-mRNAs and edges for their interactions (Figure 4). Of the 84 DE-mRNAs in the PPI network, 63 were upregulated and 21 were downregulated.

3.4. Module Analysis and Hub DE-mRNAs Identification. We applied the MCODE Cytoscape plug-in to determine the network's top module of the PPI network. The most significant module with an MCODE score of 45.872 was

https://doi.org/10.1021/acsomega.4c00011
ACS Omega 2024, 9, 24379−24395

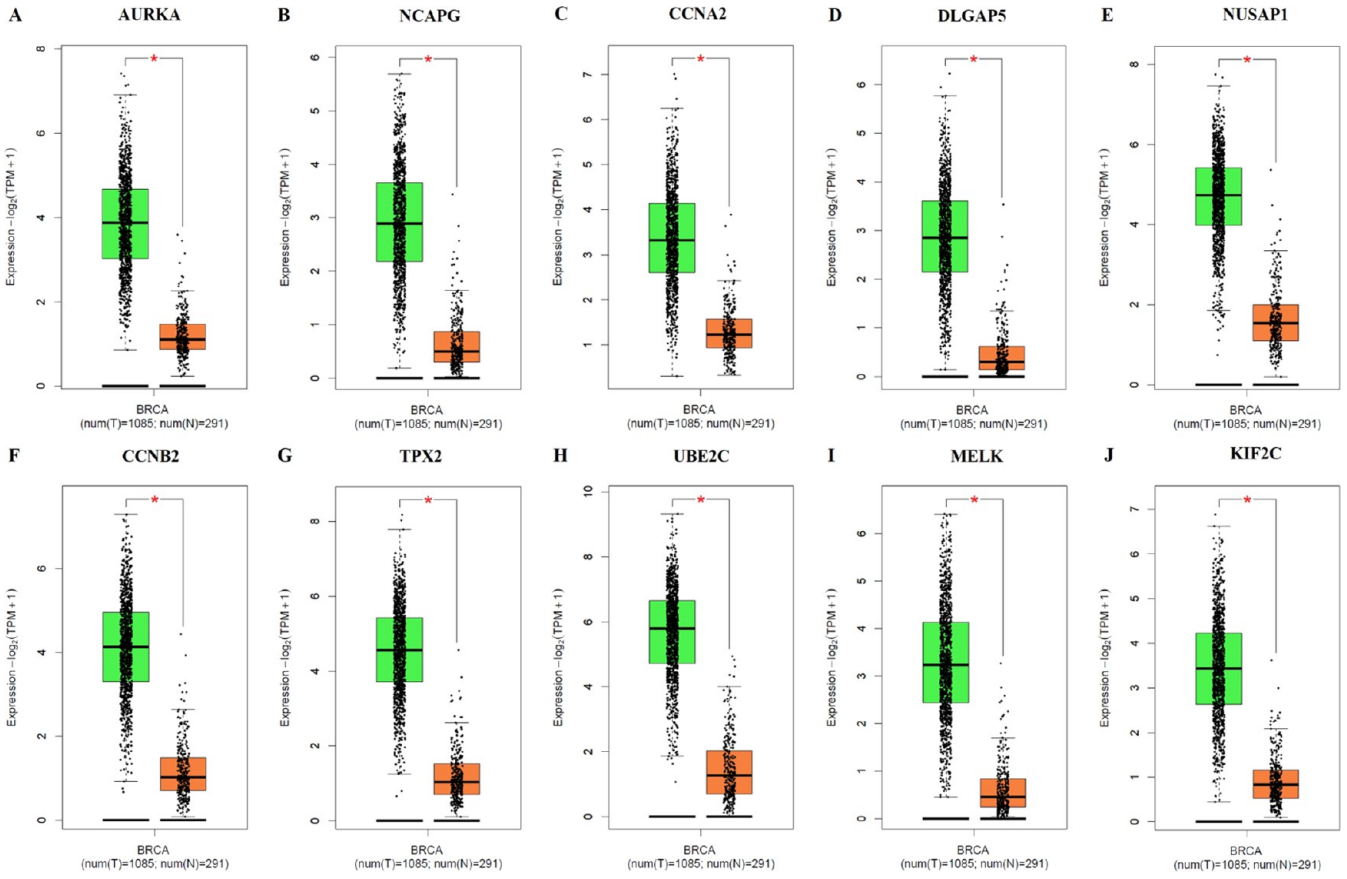

Figure 6. Expression profile of the 10 DE-mRNAs in TCGA-BRCA. (A) AURKA, (B) NCAPG, (C) CCNA2, (D) DLGAP5, (E) NUSAP1, (F) CCNB2, (G) TPX2, (H) UBE2C, (I) MELK, and (J) KIF2C. The green box represents the tumor (T), and the orange box represents normal (N).

obtained using MCODE analysis. Module 1 comprises 48 nodes and 1078 edges, including 45 upregulated DE-mRNAs and three downregulated DE-mRNAs (Figure 5A). Additionally, module 1 was subjected to the CytoNCA plug-in, which used four different algorithms, Betweenness, Closeness, eigenvector, and LAC, and identified 19 significant DE-mRNAs. Similarly, module 1 was subjected to the CytoHubba plug-in, which used four different algorithms, EPC, MCC, MNC, and Stress, and found 14 significant DE-mRNAs. We found 10 significant hub-upregulated DE-mRNAs by overlapping CytoNCA and CytoHubba (Figure 5B). We employed TCGA data via the GEPIA2 database to validate the significance of the 10 DE-mRNAs, including AURKA, NCAPG, CCNA2, DLGAP5, NUSAP1, CCNB2, TPX2, UBE2C, MELK, and KIF2C. A box plot was generated to demonstrate the mRNA expression levels, utilizing data from the TCGA-BRCA database within GEPIA2. The expression profile of 10 DE-mRNAs aligned with p-values <0.05, indicating statistical significance. Our analysis revealed significant differences between normal and tumor tissue expressions (Figure 6). OncoLnc analyzed the 10 DE-mRNAs, and results showed that CCNB2, UBE2C, MELK, and KIF2C were significantly associated with worsened survival ($p \leq 0.05$) (Figure 7).

3.5. Prediction of Hub DE-mRNAs-Associated miRNAs. The 10 significant hub-upregulated DE-mRNAs were uploaded in mirDIP to identify the miRNAs that target these mRNAs. The minimum score class to identify the associated miRNAs was set to a very high class (Top 1%) in the mirDIP web server. We visualized the obtained DE-mRNAs-miRNAs from mirDIP with Cytoscape software. We found the DE-mRNA-associated miRNA network for BC, including TNBC, which consists of 77 miRNAs and 10 DE-mRNAs (Figure 8). Furthermore, we validated the obtained DE-mRNAs-miRNAs link using the TNBC GEO data set to identify the overlapping DE-mRNAs-miRNAs in TNBC and BC. We utilized the GSE45498 data set consisting of 165 TNBC patient tumor samples and 59 adjacent normal samples to correlate and validate our results. The GSE45498 data set was generated from the GPL16231 platform for DE-miRNAs and the GPL16299 platform for DE-mRNAs. We found the DE-miRNAs between the TNBC patients and normal controls via the GEO2R tool. We obtained the significant DE-miRNAs with the cutoff values of |log2FC| 0.05 ≥ and ≤ −0.05 with p-values ≤0.05, as represented in the volcano plot (Figure 9A). We also tabulated the top 242 DE-miRNAs in Table S1. Likewise, we found the DE-mRNAs between the TNBC patients and normal controls via the GEO2R tool in GSE45498. From this, we found the significant DE-mRNAs in TNBC with cutoff values of |log2FC| +1 ≥ or ≤ −1 and p-values ≤0.05 (Figure 9B). We also tabulated the top 236 DE-mRNAs in Table S2. We overlapped the hub DE-mRNA-miRNA with GSE45498-miRNA and found five common miRNAs (Figure 9C). However, we identified four key miRNAs by cross-referencing the upregulated miRNAs with their corresponding downregulated mRNAs and vice versa: downregulated miRNAs with upregulated mRNAs. These four miRNAs' corresponding hub DE-mRNAs are listed in Table 1. Likewise, we overlapped the hub DE-mRNA with GSE45498-mRNA and found one common mRNA, CCNA2 (Figure 9D).

https://doi.org/10.1021/acsomega.4c00011
ACS Omega 2024, 9, 24379−24395

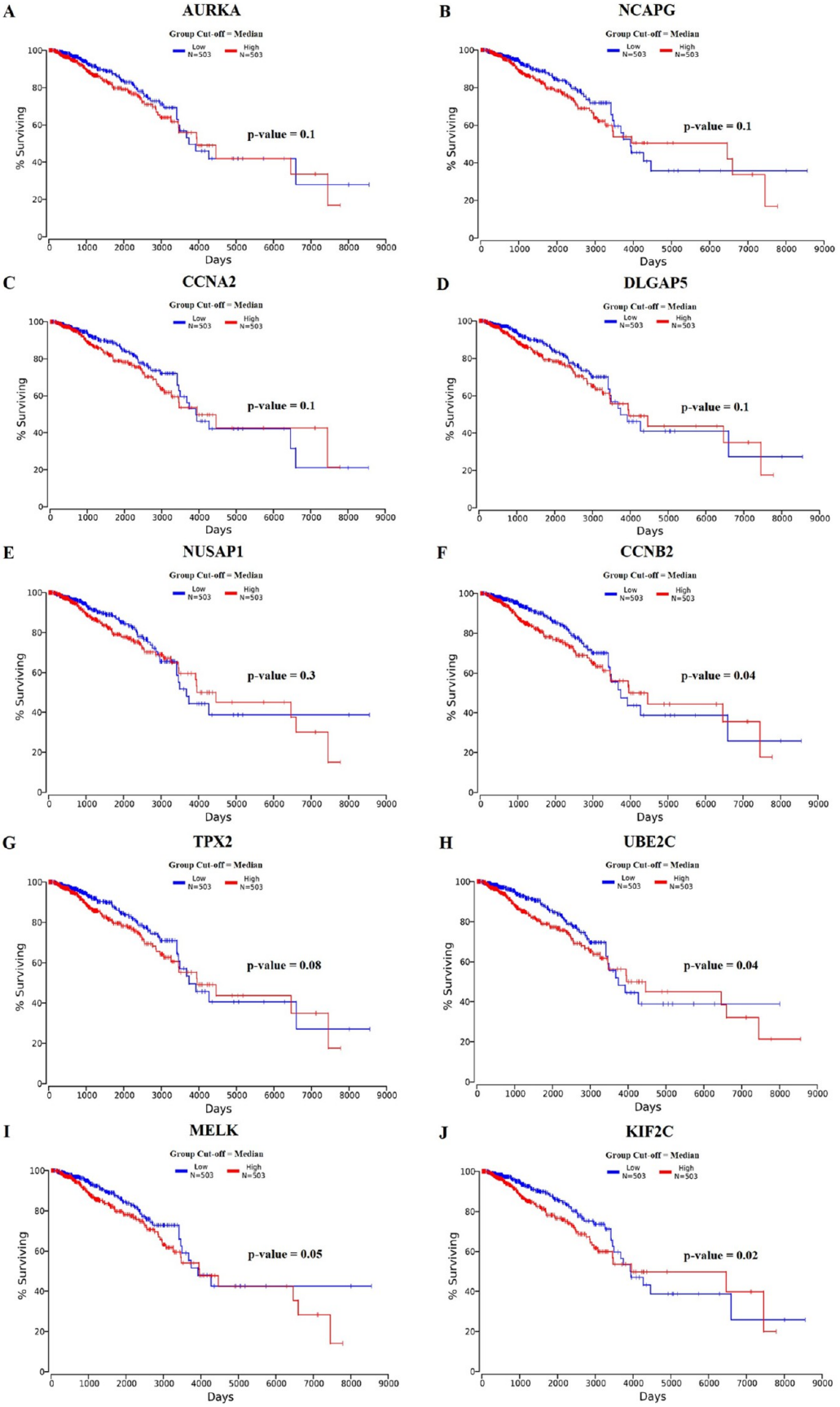

Figure 7. Overall survival analysis Kaplan−Meier plot of the 10 DE-mRNAs in TCGA-BRCA. (A) AURKA, (B) NCAPG, (C) CCNA2, (D) DLGAP5, (E) NUSAP1, (F) CCNB2, (G) TPX2, (H) UBE2C, (I) MELK, and (J) KIF2C.

https://doi.org/10.1021/acsomega.4c00011
ACS Omega 2024, 9, 24379−24395

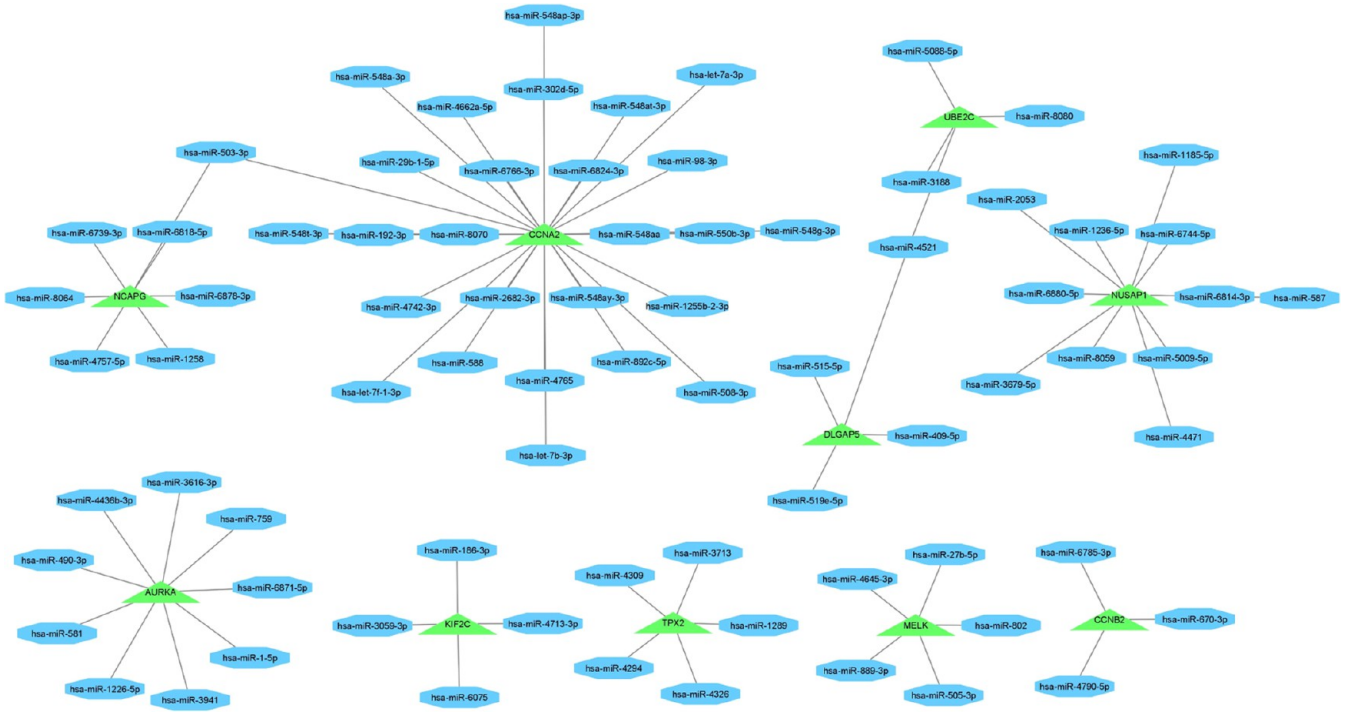

Figure 8. DEGs-miRNAs network of 10 hub DE-mRNAs attained from mirDIP and visualized in Cytoscape software. The green triangle represents the DE-mRNAs, and the blue octagon represents miRNAs.

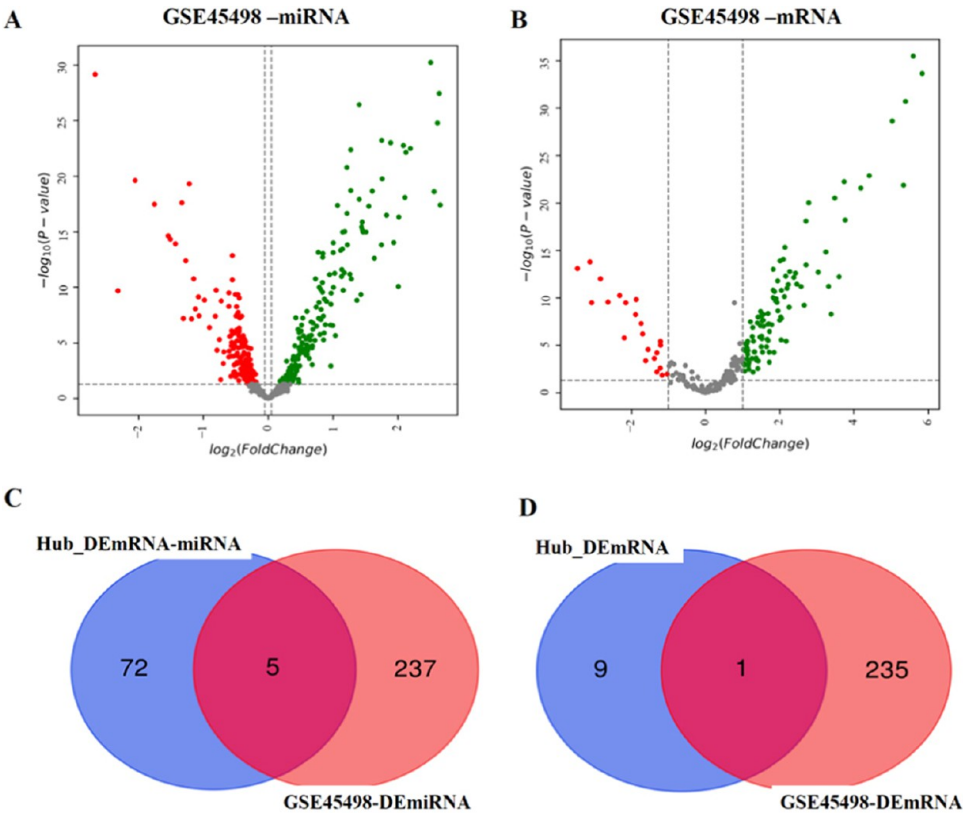

Figure 9. (A) Volcano plot of GSE45498 representing the DE-miRNAs of TNBC with the cutoff values of |log2FC| +0.05 ≥ or ≤ −0.05 and *p*-values ≤0.05. The red dot indicates downregulated DE-miRNAs, while the green dot indicates upregulated DE-miRNAs. (B) Volcano plot of GSE45498 representing the DE-mRNAs of TNBC with cutoff values of |log2FC| + 1≥ or ≤ −1 and *p*-values ≤0.05. The red dot indicates downregulated DE-mRNAs, while the green dot indicates upregulated DE-mRNAs. (C) Venn diagram showing 5 overlapped DE-miRNAs between hub DE-mRNAs-associated miRNAs and GSE45498-miRNAs. (D) Venn diagram showing one overlapped DE-mRNA between the hub DE-mRNA and GSE45498-DE-mRNAs.

https://doi.org/10.1021/acsomega.4c00011
ACS Omega 2024, 9, 24379−24395

Table 1. List of Four Significant DE-miRNAs' Corresponding Hub DE-mRNAs

sl. no.	GSE45498-DE -miRNAs	hub DE-mRNAs of corresponding miRNA
1	↓ hsa-miR-802	↑ MELK
2	↓ hsa-miR-1258	↑ NCAPG
3	↓ hsa-miR-548a-3p	↑ CCNA2
4	↓ hsa-miR-2053	↑ NUSAP1

3.6. Validation of DE-mRNAs in BC Subclasses. The expression of four hub DE-mRNAs in BC compared to its subclasses and normals using TCGA and GTEx data sets was validated using UALCAN. We examined the expressions of hub DE-mRNAs based on the BC major subclasses. MELK, NCAPG, CCNA2, and NUSAP1 expressions were noticeably higher in subclasses of BC than in normal (Figure 10). The statistically significant expression of MELK, NCAPG, CCNA2, and NUSAP1 in BC with $p < 0.05$. MELK, NCAPG, CCNA2, and NUSAP1 expression were greater in TNBC > HER2-positive > Luminal > normal subclasses. Our findings were supported by the patterns observed for these four mRNAs in the TCGA data. Additionally, immunohistochemistry staining retrieved from the HPA database revealed dysregulation in the expression of these four mRNAs (Figure 11).

3.7. Validation of DE-miRNAs. The expression levels of four hub DE-miRNAs in BC compared to those in normal tissue were validated using UALCAN with TCGA-BRCA data. Among these four, only hsa-miR-1258 was found in TCGA-BRCA, while data for the other miRNAs were insufficient to generate expression profiles. Our analysis revealed that hsa-miR-1258 was downregulated in the tumor (Figure 12A). Additionally, the survival analysis Kaplan−Meier plot for hsa-miR-1258 obtained from the OncoLnc database revealed that the low hsa-miR-1258 expression has survival rates significantly lower compared to those with high miRNA expression in breast cancer. Low miRNA expression may be associated with a poorer prognosis or shorter survival time (Figure 12B).

3.8. Functional Enrichment Analysis of DE-miRNAs. In DIANA tools, we performed functional enrichment analysis for hub DE-miRNAs of BC, including TNBC. The BP, MF, and KEGG pathway analysis for DE-miRNAs revealed significantly enriched processes/pathways with $p < 0.05$ (Figure 13). The top 10 significant biological processes of four DE-miRNAs were the cellular nitrogen compound metabolism (GO:0034641), process resulting in protein modification (GO:0006464), symbiosis (GO:0044403), biosynthesis (GO:0009058), gene expression (GO:0010467), viral process (GO:0016032), stress response (GO:0006950), neurotrophin TRK receptor signaling pathway (GO:0048011), biological_-process (GO:0008150), and catabolic process (GO:0009056) (Figure 13A). The top 10 significantly enriched molecular functions of four DE-miRNAs were enzyme binding (GO:0019899), poly-A RNA binding (GO:0003723), molecular function (GO:0003674), ion binding (GO:0043167), poly(A) RNA binding (GO:0044822), nucleic acid binding transcription factor activity (GO:0001071) activin receptor

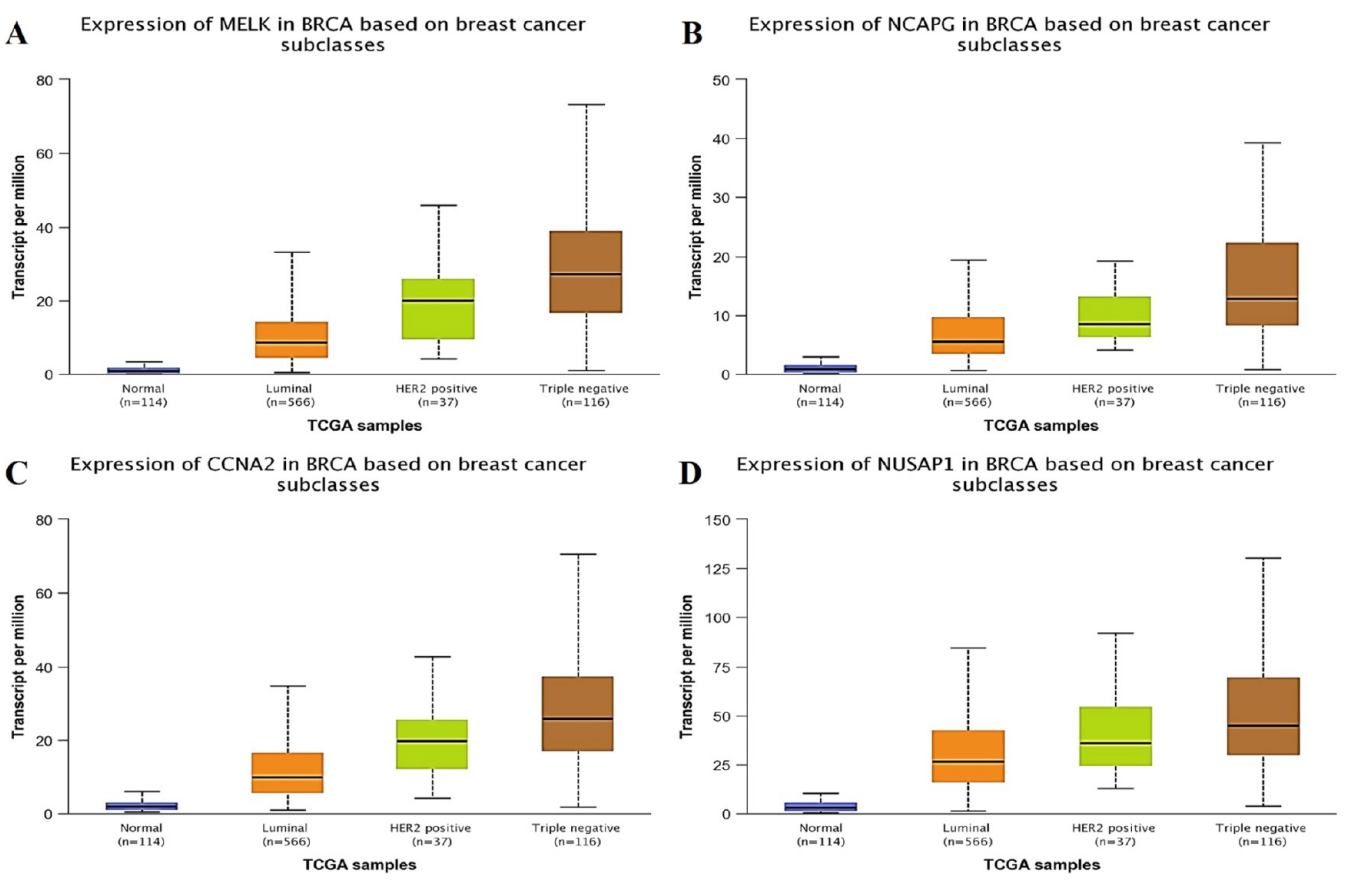

Figure 10. Box plot demonstrating the expression levels of four significant DE-mRNAs between the BC subclasses and normal samples. The expression levels of (A) MELK, (B) NCAPG, (C) CCNA2, and (D) NUSAP1 were significantly higher in all subclasses of BRCA in the TCGA database than in normal samples.

https://doi.org/10.1021/acsomega.4c00011
ACS Omega 2024, 9, 24379−24395

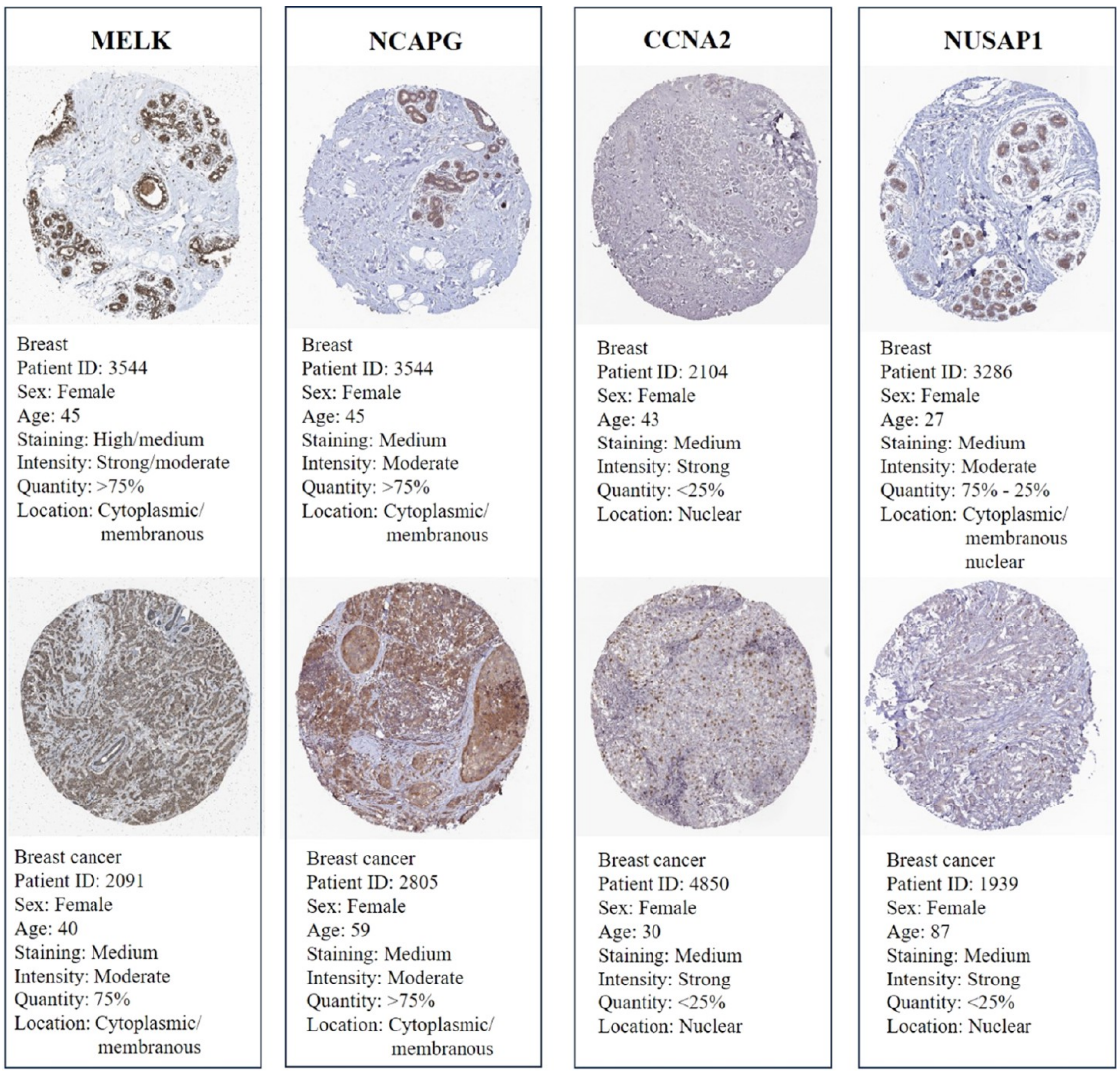

Figure 11. Validation of the mRNA/protein expression levels for the four DE-mRNAs through immunohistochemistry (IHC) data from the Human Protein Atlas database.

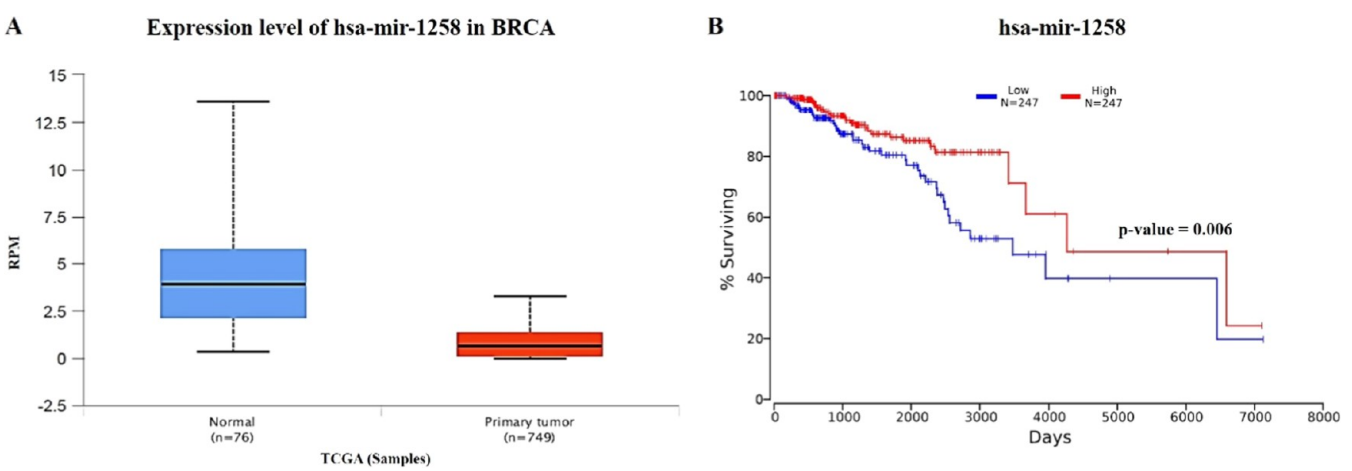

Figure 12. (A) Expression profile and (B) survival analysis (Kaplan−Meier plot) for hsa-mir-1258 using TCGA-BRCA data via the OncoLnc database.

activity, type II (GO:0016362), protein binding transcription factor activity (GO:0000988), phosphokinase activity (GO:0016301), and small conjugating protein binding (GO:0032182) (Figure 13B). The top 5 significant KEGG pathways of four DE-miRNAs were Prion diseases (hsa05020), ECM−receptor interaction (hsa04512), small-cell lung cancer

https://doi.org/10.1021/acsomega.4c00011
ACS Omega 2024, 9, 24379−24395

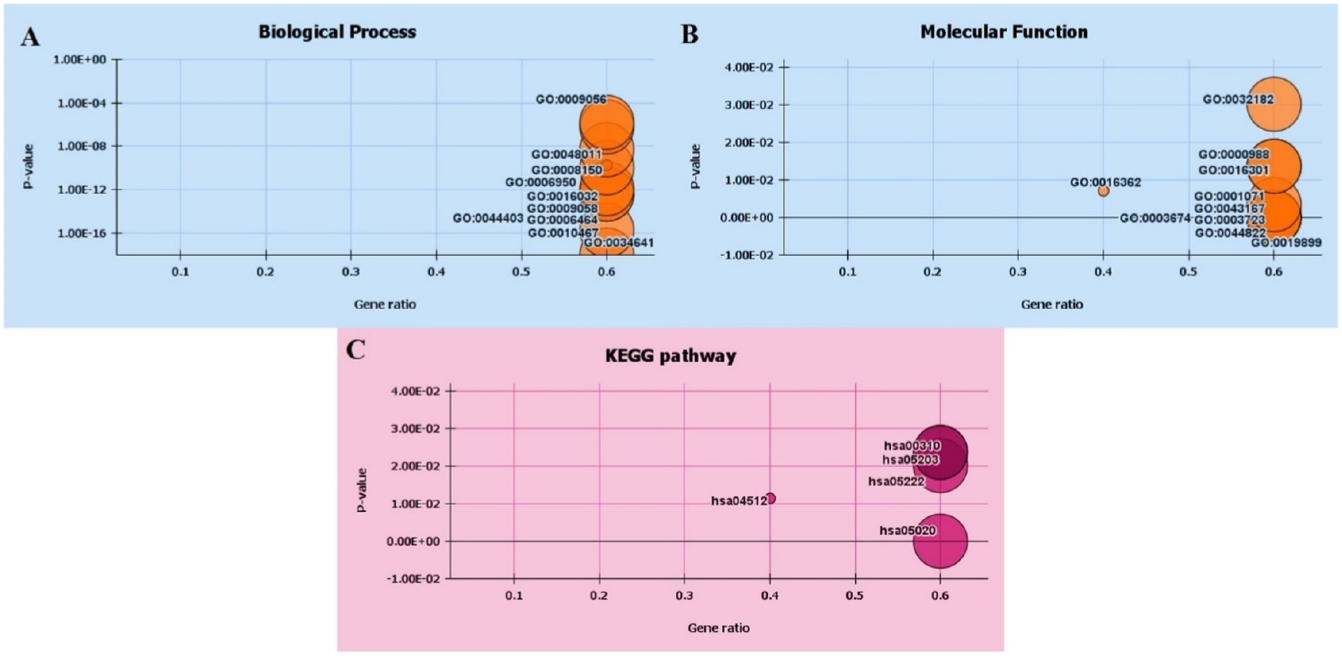

Figure 13. Functional enrichment analysis of four significant DE-miRNAs associated with TNBC. A bubble indicates a GO term, with the size of the bubble representing the number of genes in the GO term. The *X*-axis represents the gene ratio, and the *Y*-axis represents the p-value. (A) Top 10 significant biological processes of DE-miRNAs. (B) Top 10 significantly enriched molecular functions of DE-miRNAs. (C) Top 5 significant KEGG pathways of DE-miRNAs.

(hsa05222), lysine degradation (hsa00310), and viral carcinogenesis (hsa05203) (Figure 13C).

4. DISCUSSION

Breast cancer is linked with a high death rate in females, and the incidence is rising globally.[23] The most lethal subtype of breast cancer is TNBC. Options for treating TNBC are rather limited. Advanced stages of this cancer are predominantly managed through chemotherapy. It is believed that complex signaling networks govern the development of TNBC, and understanding its precise molecular process might lead to the creation of effective therapies and novel prognostic biomarkers.[24] miRNAs carried by exosomes from the tumor represent a promising new class of breast cancer biomarkers. miRNAs are one type of noncoding RNA that are thought to be master modulators of cancer phenotype because they control mRNA expression levels.[25,26]

We discovered 159 communal DE-mRNAs, including 78 upregulated and 81 downregulated mRNAs in TNBC, BC with ER+/ER− and TCGA-BRCA, by comprehensively analyzing GSE42568, GSE185645, and TCGA. These communal DE-mRNAs were subjected to GO BP, MF, and KEGG pathway annotations. The DE-upregulated mRNAs were mainly enriched in BP, such as cell division, mitotic spindle organization, and mitotic cell cycle, and MF, such as protein binding and microtubule binding. The KEGG pathways showed that the DE-mRNAs were mainly enriched pathways such as the cell cycle, oocyte meiosis, and cellular senescence.

We built a PPI network via STRING and Cytoscape for 159 common DE-mRNAs, including 78 upregulated and 81 downregulated. Later, we subjected the PPI network for MCODE, CytoHubba, and CytoNCA and identified the 10 hub DE-mRNAs: AURKA, NCAPG, CCNA2, DLGAP5, NUSAP1, CCNB2, TPX2, UBE2C, MELK, and KIF2C.

According to previous research, AURKA interacts with and phosphorylates many crucial proteins involved in stress response and cell cycle checkpoint following DNA damage.[27] *AURKA* overexpression caused checkpoint deficiencies and genomic instability, which eventually aided in the onset progression of cancer. It also decreased transcriptional activity and increased *p53* degradation.[28] In breast cancer stem cells, AURKA interacts with METTL14 by inhibiting its ubiquitination and degradation. This degradation leads to METTL14 stabilization and promotes methylation of the DROSHA transcript. AURKA then activates modification by N^6-methyladenosine (m^6A), which further promotes stability in the DROSHA transcript, which reacts to *β*-Catenin to transactivate STC1 independent of RNA cleavage, leading to the promotion of breast cancer stem cell-like properties.[29−31] BC and TNBC patients' survival was substantially correlated with high *AURKA* expression.[32−34]

The evidence from experimental investigations has clearly established that the *NCAPG* gene and its corresponding mRNA are expressed at significantly elevated levels in breast cancer cells compared to normal cells. NCAPG exhibits a negative correlation with estrogen receptor (ER) and progesterone receptor (PR) expression but presents a somewhat positive correlation with human epidermal growth factor receptor 2 (HER2) expression. Despite this, ER and PR may still demonstrate extremely low expression levels. In relevance to breast cancer, *NCAPG* gene expression is regulated by four miRNAs (miR-195-5p, miR-101-3p, miR-944, and miR-214-3p) and 12 coexpressed genes by interacting with the p53 signaling pathway.[35,36] Additionally, it was noted that high *NCAPG* expression is linked to a bad prognosis for various tumor types, and its overexpression may be crucial for controlling tumor-related pathways during tumor growth.[37]

Cyclin A2, called *CCNA2*, is irregularly expressed in cervical, colorectal, and breast cancers. It is expressed significantly in

https://doi.org/10.1021/acsomega.4c00011
ACS Omega 2024, 9, 24379−24395

tissues with TNBC compared with other adjacent tissues. CCNA2 protein is more abundantly expressed in MDA-MB-468 and MDA-MB-231 cell lines than all other breast cancer cell lines, thus, making them often used for research studies. MDA-MB-231 and MDA-MB-468 cells were considered TNBC/basal-B mammary carcinoma and TNBC/basal-A mammary carcinoma, respectively.[38,39] Most cancer types expressed CCNA2 differently from healthy tissues—the prognosis of several cancers, particularly clear cell renal carcinoma (ccRCC).[40]

DLGAP5 transcript increases in breast cancer tissues, leading to overexpression of HER2. DLGAP5 is connected to the Aurora signal transduction pathway, including its phosphoprotein phosphate activity. Tissues from breast cancer cases exhibited elevated levels of DLGAP5. Furthermore, the status and stages of lymph nodes were correlated with the expression levels. The elevated DLGAP5 expression levels were linked to a poor prognosis. Further, they reported that DLGAP5 could serve as a putative autophagy receptor in mitophagy.[41] DLGAP5 is also linked to the prognosis of non-small-cell lung cancer, prostate cancer, gastric cancer, and colorectal cancer.[42−47]

TPX2 is increased in patients with overexpression of *HER2*. This *TPX2* expression reduces the survival rate of patients with a very high *HER2* expression. *TPX2* increases rather gradually than abruptly. That is, it increases gradually with the progressive stages of BC.[48] A previous study revealed that an increased *TPX2* expression level usually happens in the presence of *TP53* mutation and high ploidy. A significant association exists between *TPX2* expression in nuclear and aggressive tumor behavior in large breast cancer cohorts.[49]

NUSAP1 is taking part in the development, progression, and metastasis and advanced stages of cancer. *NUSAP1* was significantly overexpressed and promoted cancer development in the MCF-7 cell lines. It was also overexpressed in MDA-MB-231 BC cell lines and showed comparatively lower expression in BT-474 cell lines. BT-474 cell line is a BC cell line with an increased expression of HER2 and ER, whereas MDA-MB-231 is a TNBC cell line, which is most aggressive, invasive, and poorly distinguished since it lacks receptor expression of ER, PR, and HER2.[50] *NUSAP1* expression is also seen in cancers with positive expression of two receptors, ER+ and PR+. *NUSAP1* expression is pointedly higher in ductal carcinoma in situ than in invasive ductal carcinoma, which is higher than in other BC tissue types. In BC cells, NUSAP1 increases cell growth and metastasis of the cancer-affected cells by targeting the AMPK/PPARγ pathway.[51]

The downregulation of *CCNB2* leads to the inhibition of cell proliferation and enhancement of cell cycle arrest in the G2/M phase of the cell cycle; its mutation and defects often lead to cancer development. Therefore, overexpression of *CCNB2* is found in BC tissues. *CCNB2* expression is predominantly higher in patients with TNBC. On conducting gene expression experiments on shRNA plasmid transfection in MDA-MB-231 and HCC-1937 cells, the depletion of *CCNB2* gene expression led to a decrease in the colony number of the BC tissues,[52] suggesting that TNBC cell growth in vitro was aided by CCNB2.

Higher expression of *UBE2C* leads to an increase in the severity of BC. During *UBE2C* gene knockdown experiments, a significant reduction in mRNA expression of UBE2C, leading to lower cancer invasion, can be seen in MCF-7 and MDA-MB-231 cells. *UBE2C* gene targets the AKT/mTOR signaling pathway to induce cancer development and invasion. Thus, *UBE2C* gene expression inhibition leads to inhibition of the AKT/mTOR signaling pathway and suppression of spreading BC.[53] UBE2C expression is higher in patients with TNBC, patients with amplified expression of HER2, and patients with luminal cancers. It is majorly high in infiltrating lobular and infiltrating ductal carcinoma. In urologic cancer, high expression of UBE2C was seen in papillary (papillary type 1 and papillary type 2) and nonpapillary tumors compared to normal tissues.[54]

Overexpression of the *MELK* gene was observed in patients with BC, leading to a poor prognosis. On ablation of the *MELK* gene, proliferation was selectively inhibited in patients with basal-like BC. However, it was later found that *MELK* gene expression did not significantly inhibit proliferation in basal-like breast cancers. This concluded its complex role in breast cancers.[55,56] *MELK* is thus overexpressed in patients with BC compared to those in normal tissues. In BC, *MELK* gene expression is significantly upregulated due to the binding of a cancer-promoting competing endogenous RNA (ceRNA), namely, PCDHB17P, to miR-145-3p, leading to its inability to bind to the *MELK* gene and inhibit it. MiR-145-3p directly targets the *MELK* gene and inhibits its expression. Thus, *MELK* is overexpressed and thus causes cancer. Moreover, the promoter activity and PCDHB17P expression can be increased by MELK through NF-κB, creating a positive feedback loop that leads to metastasis and angiogenesis in BC.[57]

In knockdown experiments on *KIF2C*, the proliferation of BC cells is inhibited by various biological processes like restoring ciliation, G2/M phase arrest, deregulating cell division, and delayed exit from mitosis.[58] In individuals with BC, the mRNA and protein levels of KIF2C are elevated. KIF2C is also significantly upregulated in lung adenocarcinoma and is associated with its progression and recurrence.[59] It is also seen to be overexpressed in several cancers like breast, lung, colon, bladder, skin, blood, liver, soft tissue, and other cancers.[60]

Additionally, we validated hub DE-mRNAs associated miRNAs link using the TNBC GEO data set GSE45498DE-miRNAs by overlapping and identified four significant downregulated miRNAs, namely, hsa-miR-802, hsa-miR-1258, hsa-miR-548a-3p, and hsa-miR-2053. Functional enrichment analysis identified the significant functions and pathways associated with these four DE-miRNAs, as illustrated in Figure 9.

In our study, hsa-miR-802 expression was downregulated in TNBC, which may be associated with the overexpression of MELK. hsa-miR-802 expression was considerably downregulated in patients with BC compared with the adjacent normal breast epithelial tissues. miR-802 overexpression leads to significant downregulation in the gene expression level of Forkhead box protein M1 (FoxM1), an oncogene with a potential miR-802 binding site, thus reducing the cell growth activity of BC cells.[61]

miR-1258 expression was considerably downregulated in BC cells, leading to low survival rates in patients with low miR-1258 gene expression. Breast cancer tissues have low miR-1258 expression and high expression of *E2F1*. miR-1258 overexpression would lead to the inhibition of *E2F1*, further inhibiting cell growth, blocking the cell cycle in the G0/G1 phase, and promoting cell death. *E2F1* is significantly overexpressed in Breast Cancer cell lines.[62] We observed that

https://doi.org/10.1021/acsomega.4c00011
ACS Omega 2024, 9, 24379−24395

downregulated miR-1258 expression in TNBC may lead to the overexpression of *NCAPG*.

EXT1 is identified as a potential target for hsa-mir-490-3p. Since significantly increased expression of *EXT1* and *EXT2* can be seen in lung squamous cell carcinoma (LUSC). At the same time, *EXT1* also causes poor prognosis in patients with LUSC; hsa-mir-490-3p can be used to therapeutically target patients with LUSC. It was also found that the level of hsa-mir-490-3p expression was considerably downregulated in LUSC patients. Thus, its upregulation may promote the knockdown of the *ETX1* gene, which further leads to the inhibition of cancer development.[63] hsa-mir-490-3p expression is linked with tumorigenesis of many different human cancers like colorectal cancer, glioma, prostate cancer, esophageal squamous cell carcinoma, hepatocellular carcinoma, etc.[64−69]

An earlier investigation revealed that DDR2 might interact with the mitochondrial subunits hsa-mir-548a-3p. Additionally, they claimed that DDR2 was likely to control mitochondrial activity and serve as a novel biomarker for BC's clinical diagnosis and prediction.[70]

The downregulated hsa-miR-2053 increases KIF3C expression and activates the PI3K/AKT signaling pathway, causing esophageal cancer cells to proliferate, undergo apoptosis, migrate, and invade.[71] A previous study revealed that hsa-miR-2053 expression is upregulated in patients with malignant pleural mesothelium (MPM). Further, they concluded that hsa-miR-2053 is an independent prognostic factor of MPM.[72] The upregulated miR-1258 associated with CRC directly targeting E2F8 controls the cell cycle and inhibits cell growth.[73]

These four DE-miRNAs associated mRNAs, such as MELK, NCAPG, CCNA2, and NUSAP1, were further validated in UALCAN for their mRNAs expression level in BC subclasses. The resulting expression of MELK, NCAPG, CCNA2, and NUSAP1 was significantly greater in TNBC than in other subclasses. Four crucial miRNAs were pinpointed by correlating downregulated miRNAs with their upregulated mRNA counterparts, and vice versa. Table 1 lists the hub DE-mRNAs corresponding to these four miRNAs. According to recent studies, circKIF4A has a part in brain metastasis in TNBC. Modifying the circKIF4A/miR-637/STAT3 axis functions as an oncogene.[74] Dysregulation of miRNAs, in either expression or function, can result in abnormal control of target mRNAs, playing a role in the onset and advancement of various diseases, including cancer. Our study identified important miRNA−mRNA interactions, including hsa-miR-802/MELK, hsa-miR-1258/NCAPG, miR-548a-3p/CCNA2, and hsa-miR-2053/NUSAP1, in both BC and TNBC. These findings shed light on potential regulatory mechanisms underlying these cancer types. However, further research is imperative to validate the functional significance of these interactions, providing insights into their roles in BC and TNBC progression and potentially forming the development of novel therapeutic strategies. Similarly, we overlapped the hub DE-mRNA with GSE45498-mRNA and identified a common CCNA2 DE-mRNA expression. We conducted validation of the expression of CCNA2 in TCGA-BRCA, revealing elevated levels in BC cases. However, survival analysis indicated that this increased expression does not necessarily correlate with a worsening patient prognosis. This underscores the complexity of cancer biology and suggests that CCNA2 may not be a significant prognostic factor in BC.

Further investigation is needed to elucidate the precise role of CCNA2 in BC progression and to identify alternative prognostic markers that may better inform patient outcomes and guide treatment strategies. We also pinpointed four DE-miRNAs that exhibit downregulation in BC, including TNBC. However, due to inadequate data on these miRNAs in TCGA-BRCA, our evaluation focused solely on hsa-miR-548a-3p. Our analysis revealed decreased expression, which is associated with poor overall survival in BC patients. We identified 10 significantly overexpressed DE-mRNAs in various breast cancer subtypes, including AURKA, NCAPG, CCNA2, DLGAP5, NUSAP1, CCNB2, TPX2, UBE2C, MELK, and KIF2C. Notably, CCNB2, UBE2C, MELK, and KIF2C were associated with worsened survival outcomes according to OncoLnc Kaplan−Meier analysis. Future investigations are crucial to decipher the roles and mechanisms of these DE-mRNAs in breast cancer progression, potentially uncovering novel therapeutic targets and prognostic biomarkers to guide personalized treatment strategies.

5. CONCLUSIONS

Our study identified key miRNA−mRNA interactions such as hsa-miR-802/MELK, hsa-miR-1258/NCAPG, hsa-miR-548a-3p/CCNA2, and hsa-miR-2053/NUSAP1 in both BC and TNBC, shedding light on potential regulatory mechanisms. While CCNA2 expression was elevated in BC cases, survival analysis did not correlate it with worsened prognosis, suggesting its complex role in BC. Additionally, hsa-miR-548a-3p downregulation was associated with poor overall survival in BC patients. Furthermore, four significantly overexpressed DE-mRNAs, including CCNB2, UBE2C, MELK, and KIF2C, were linked to worse survival outcomes. Further research is needed to understand their roles and identify possible therapeutic targets for BC.

■ ASSOCIATED CONTENT

Supporting Information

The Supporting Information is available free of charge at https://pubs.acs.org/doi/10.1021/acsomega.4c00011.

List of the top 242 DE-miRNAs and top 236 DE-mRNAs in TNBC samples from the GSE45498 data set. (PDF)

■ AUTHOR INFORMATION

Corresponding Author

George Priya C. Doss − *Laboratory of Integrative Genomics, Department of Integrative Biology, School of BioSciences and Technology, Vellore Institute of Technology, Vellore 632014 Tamil Nadu, India;* orcid.org/0000-0002-5971-8290; Email: georgepriyadoss@vit.ac.in

Authors

Ambritha Balasundaram − *Laboratory of Integrative Genomics, Department of Integrative Biology, School of BioSciences and Technology, Vellore Institute of Technology, Vellore 632014 Tamil Nadu, India*

Tanisha Saurav Mitra − *Laboratory of Integrative Genomics, Department of Integrative Biology, School of BioSciences and Technology, Vellore Institute of Technology, Vellore 632014 Tamil Nadu, India*

Iftikhar Aslam Tayubi − *Department of Computer Science, Faculty of Computing and Information Technology, Rabigh*

https://doi.org/10.1021/acsomega.4c00011
ACS Omega 2024, 9, 24379−24395

(FCITR), King Abdulaziz University, Jeddah 21589, Saudi Arabia

Hatem Zayed − *Department of Biomedical Sciences, College of Health Sciences, QU Health, Qatar University, Doha 2713, Qatar;* orcid.org/0000-0001-8838-6638

Complete contact information is available at: https://pubs.acs.org/10.1021/acsomega.4c00011

Author Contributions

A.B. and G.P.C.D. were involved in the study's design. A.B. and I.A.T. were involved in the data collection, experimentation, acquisition of results, and analysis. A.B., I.A.T., and T.S.M. were involved in interpreting the results and drafting the manuscript. G.P.C.D., and H.Z. supervised the entire study, were involved in acquiring, analyzing, and understanding the data, and critically reviewed the manuscript. All authors edited and approved the submitted version of the article.

Notes

The authors declare no competing financial interest.

■ ACKNOWLEDGMENTS

A.B. gratefully acknowledges the Indian Council of Medical Research (ICMR), India, for providing Senior Research Fellowship [BMI/11(05)/2022]. The authors thank the management of Vellore Institute of Technology (VIT), Vellore, Tamil Nadu, India, for providing the necessary facilities and encouragement to carry out this work.

■ REFERENCES

(1) Huang, M.; Haiderali, A.; Fox, G. E.; Frederickson, A.; Cortes, J.; Fasching, P. A.; O'Shaughnessy, J. Economic and Humanistic Burden of Triple-Negative Breast Cancer: A Systematic Literature Review. *Pharmacoeconomics* **2022**, *40* (5), 519−558.

(2) Chlebowski, R. T.; Chen, Z.; Anderson, G. L.; Rohan, T.; Aragaki, A.; Lane, D.; Dolan, N. C.; Paskett, E. D.; McTiernan, A.; Hubbell, F. A.; Adams-Campbell, L. L.; Prentice, R. Ethnicity and Breast Cancer: Factors Influencing Differences in Incidence and Outcome. *J. Natl. Cancer Inst.* **2005**, *97* (6), 439−448.

(3) Sung, H.; Ferlay, J.; Siegel, R. L.; Laversanne, M.; Soerjomataram, I.; Jemal, A.; Bray, F. Global Cancer Statistics 2020: GLOBOCAN Estimates of Incidence and Mortality Worldwide for 36 Cancers in 185 Countries. *Ca, Cancer J. Clin.* **2021**, *71* (3), 209−249.

(4) Sharma, G. N.; Dave, R.; Sanadya, J.; Sharma, P.; Sharma, K. K. Various Types and Management of Breast Cancer: An Overview. *J. Adv. Pharm. Technol. Res.* **2010**, *1* (2), 109−126.

(5) Makki, J. Diversity of Breast Carcinoma: Histological Subtypes and Clinical Relevance. *Clin Med. Insights Pathol.* **2015**, *8*, 23−31.

(6) Foulkes, W. D.; Smith, I. E.; Reis-Filho, J. S. Triple-Negative Breast Cancer. *N. Engl. J. Med.* **2010**, *363* (20), 1938−1948.

(7) Li, Y.; Kong, X.; Wang, Z.; Xuan, L. Recent Advances of Transcriptomics and Proteomics in Triple-Negative Breast Cancer Prognosis Assessment. *J. Cell. Mol. Med.* **2022**, *26* (5), 1351−1362.

(8) Malorni, L.; Shetty, P. B.; De Angelis, C.; Hilsenbeck, S.; Rimawi, M. F.; Elledge, R.; Osborne, C. K.; De Placido, S.; Arpino, G. Clinical and Biologic Features of Triple-Negative Breast Cancers in a Large Cohort of Patients with Long-Term Follow-Up. *Breast Cancer Res. Treat.* **2012**, *136* (3), 795−804.

(9) Ding, L.; Gu, H.; Xiong, X.; Ao, H.; Cao, J.; Lin, W.; Yu, M.; Lin, J.; Cui, Q. MicroRNAs Involved in Carcinogenesis, Prognosis, Therapeutic Resistance and Applications in Human Triple-Negative Breast Cancer. *Cells* **2019**, *8* (12), No. 1492.

(10) Kumar, P.; Aggarwal, R. An Overview of Triple-Negative Breast Cancer. *Arch. Gynecol. Obstet.* **2016**, *293* (2), 247−269.

(11) Ovcaricek, T.; Frkovic, S. G.; Matos, E.; Mozina, B.; Borstnar, S. Triple Negative Breast Cancer - Prognostic Factors and Survival. *Radiol. Oncol.* **2011**, *45* (1), 46−52.

(12) Wang, C.; Kar, S.; Lai, X.; Cai, W.; Arfuso, F.; Sethi, G.; Lobie, P. E.; Goh, B. C.; Lim, L. H. K.; Hartman, M.; Chan, C. W.; Lee, S. C.; Tan, S. H.; Kumar, A. P. Triple Negative Breast Cancer in Asia: An Insider's View. *Cancer Treat. Rev.* **2018**, *62*, 29−38.

(13) Yu, D.-d.; Lv, M.; Chen, W.; Zhong, S.; Zhang, X.; Chen, L.; Ma, T.; Tang, J.; Zhao, J. Role of miR-155 in Drug Resistance of Breast Cancer. *Tumour Biol.* **2015**, *36* (3), 1395−1401.

(14) Peng, Y.; Croce, C. M. The Role of MicroRNAs in Human Cancer. *Signal Transduction Targeted Ther.* **2016**, *1*, No. 15004.

(15) Clough, E.; Barrett, T. The Gene Expression Omnibus Database. *Methods Mol. Biol.* **2016**, *1418*, 93−110.

(16) Tang, Z.; Kang, B.; Li, C.; Chen, T.; Zhang, Z. GEPIA2: An Enhanced Web Server for Large-Scale Expression Profiling and Interactive Analysis. *Nucleic Acids Res.* **2019**, *47* (W1), W556−W560.

(17) Sherman, B. T.; Hao, M.; Qiu, J.; Jiao, X.; Baseler, M. W.; Lane, H. C.; Imamichi, T.; Chang, W. DAVID: A Web Server for Functional Enrichment Analysis and Functional Annotation of Gene Lists (2021 Update). *Nucleic Acids Res.* **2022**, *50* (W1), W216−221.

(18) Szklarczyk, D.; Gable, A. L.; Nastou, K. C.; et al. The STRING Database in 2021: Customizable Protein-Protein Networks, and Functional Characterization of User-Uploaded Gene/Measurement Sets. *Nucleic Acids Res.* **2021**, *49*, D605−D612.

(19) Doncheva, N. T.; Morris, J. H.; Gorodkin, J.; Jensen, L. J. Cytoscape StringApp: Network Analysis and Visualization of Proteomics Data. *J. Proteome Res.* **2019**, *18* (2), 623−632.

(20) Tokar, T.; Pastrello, C.; Rossos, A. E. M.; Abovsky, M.; Hauschild, A.-C.; Tsay, M.; Lu, R.; Jurisica, I. mirDIP 4.1-Integrative Database of Human microRNA Target Predictions. *Nucleic Acids Res.* **2018**, *46* (D1), D360−D370.

(21) Chandrashekar, D. S.; Bashel, B.; Balasubramanya, S. A. H.; Creighton, C. J.; Ponce-Rodriguez, I.; Chakravarthi, B. V. S. K.; Varambally, S. UALCAN: A Portal for Facilitating Tumor Subgroup Gene Expression and Survival Analyses. *Neoplasia* **2017**, *19* (8), 649−658.

(22) Vlachos, I. S.; Zagganas, K.; Paraskevopoulou, M. D.; Georgakilas, G.; Karagkouni, D.; Vergoulis, T.; Dalamagas, T.; Hatzigeorgiou, A. G. DIANA-miRPath v3.0: Deciphering microRNA Function with Experimental Support. *Nucleic Acids Res.* **2015**, *43* (W1), W460−466.

(23) Wilkinson, L.; Gathani, T. Understanding Breast Cancer as a Global Health Concern. *Br. J. Radiol.* **2022**, *95* (1130), No. 20211033.

(24) Zagami, P.; Carey, L. A. Triple Negative Breast Cancer: Pitfalls and Progress. *npj Breast Cancer* **2022**, *8* (1), 95.

(25) Baldasici, O.; Pileczki, V.; Cruceriu, D.; Gavrilas, L. I.; Tudoran, O.; Balacescu, L.; Vlase, L.; Balacescu, O. Breast Cancer-Delivered Exosomal miRNA as Liquid Biopsy Biomarkers for Metastasis Prediction: A Focus on Translational Research with Clinical Applicability. *Int. J. Mol. Sci.* **2022**, *23* (16), 9371.

(26) Jordan-Alejandre, E.; Campos-Parra, A. D.; Castro-López, D. L.; Silva-Cázares, M. B. Potential miRNA Use as a Biomarker: From Breast Cancer Diagnosis to Metastasis. *Cells* **2023**, *12* (4), 525.

(27) Marumoto, T.; Honda, S.; Hara, T.; Nitta, M.; Hirota, T.; Kohmura, E.; Saya, H. Aurora-A Kinase Maintains the Fidelity of Early and Late Mitotic Events in HeLa Cells. *J. Biol. Chem.* **2003**, *278* (51), 51786−51795.

(28) Tentler, J. J.; Ionkina, A. A.; Tan, A. C.; Newton, T. P.; Pitts, T. M.; Glogowska, M. J.; Kabos, P.; Sartorius, C. A.; Sullivan, K. D.; Espinosa, J. M.; Eckhardt, S. G.; Diamond, J. R. P53 Family Members Regulate Phenotypic Response to Aurora Kinase A Inhibition in Triple-Negative Breast Cancer. *Mol. Cancer Ther.* **2015**, *14* (5), 1117−1129.

(29) Peng, F.; Xu, J.; Cui, B.; Liang, Q.; Zeng, S.; He, B.; Zou, H.; Li, M.; Zhao, H.; Meng, Y.; Chen, J.; Liu, B.; Lv, S.; Chu, P.; An, F.; Wang, Z.; Huang, J.; Zhan, Y.; Liao, Y.; Lu, J.; Xu, L.; Zhang, J.; Sun, Z.; Li, Z.; Wang, F.; Lam, E. W.-F.; Liu, Q. Oncogenic AURKA-Enhanced N(6)-Methyladenosine Modification Increases DROSHA

mRNA Stability to Transactivate STC1 in Breast Cancer Stem-like Cells. *Cell Res.* **2021**, *31* (3), 345−361.
(30) Han, J.; Lee, Y.; Yeom, K.-H.; Kim, Y.-K.; Jin, H.; Kim, V. N. The Drosha-DGCR8 Complex in Primary microRNA Processing. *Genes Dev.* **2004**, *18* (24), 3016−3027.
(31) Gromak, N.; Dienstbier, M.; Macias, S.; Plass, M.; Eyras, E.; Cáceres, J. F.; Proudfoot, N. J. Drosha Regulates Gene Expression Independently of RNA Cleavage Function. *Cell Rep.* **2013**, *5* (6), 1499−1510.
(32) Xu, J.; et al. Aurora-A Identifies Early Recurrence and Poor Prognosis and Promises a Potential Therapeutic Target in Triple Negative Breast Cancer. *PLoS One* **2013**, *8* (2), No. e56919.
(33) Liao, Y.; Liao, Y.; Li, J.; Li, J.; Fan, Y.; Xu, B. Polymorphisms in AURKA and AURKB Are Associated with the Survival of Triple-Negative Breast Cancer Patients Treated with Taxane-Based Adjuvant Chemotherapy. *Cancer Manage. Res.* **2018**, *10*, 3801−3808.
(34) Nadler, Y.; Camp, R. L.; Schwartz, C.; Rimm, D. L.; Kluger, H. M.; Kluger, Y. Expression of Aurora A (but Not Aurora B) Is Predictive of Survival in Breast Cancer. *Clin. Cancer Res.* **2008**, *14* (14), 4455−4462.
(35) Dong, M.; Xu, T.; Cui, X.; Li, H.; Li, X.; Xia, W. NCAPG Upregulation Mediated by Four microRNAs Combined with Activation of the P53 Signaling Pathway Is a Predictor of Poor Prognosis in Patients with Breast Cancer. *Oncol. Lett.* **2021**, *21* (4), 323.
(36) Cai, X.; Gao, J.; Shi, C.; Guo, W. Z.; Guo, D.; Zhang, S. The Role of NCAPG in Various of Tumors. *Biomed. Pharmacother.* **2022**, *155*, No. 113635.
(37) Xiao, C.; Gong, J.; Jie, Y.; Cao, J.; Chen, Z.; Li, R.; Chong, Y.; Hu, B.; Zhang, Q. NCAPG Is a Promising Therapeutic Target Across Different Tumor Types. *Front. Pharmacol.* **2020**, *11*, 387.
(38) Ma, J.; Chen, C.; Liu, S.; Ji, J.; Wu, D.; Huang, P.; Wei, D.; Fan, Z.; Ren, L. Identification of a Five Genes Prognosis Signature for Triple-Negative Breast Cancer Using Multi-Omics Methods and Bioinformatics Analysis. *Cancer Gene Ther.* **2022**, *29* (11), 1578−1589.
(39) Lu, Y.; Su, F.; Yang, H.; Xiao, Y.; Zhang, X.; Su, H.; Zhang, T.; Bai, Y.; Ling, X. E2F1 Transcriptionally Regulates CCNA2 Expression to Promote Triple Negative Breast Cancer Tumorigenicity. *Cancer Biomarkers* **2022**, *33* (1), 57−70.
(40) Jiang, A.; Zhou, Y.; Gong, W.; Pan, X.; Gan, X.; Wu, Z.; Liu, B.; Qu, L.; Wang, L. CCNA2 as an Immunological Biomarker Encompassing Tumor Microenvironment and Therapeutic Response in Multiple Cancer Types. *Oxid. Med. Cell. Longevity* **2022**, *2022*, No. e5910575.
(41) Xu, T.; Dong, M.; Li, H.; Zhang, R.; Li, X. Elevated mRNA Expression Levels of DLGAP5 Are Associated with Poor Prognosis in Breast Cancer. *Oncol. Lett.* **2020**, *19* (6), 4053−4065.
(42) Branchi, V.; García, S. A.; Radhakrishnan, P.; Győrffy, B.; Hissa, B.; Schneider, M.; Reißfelder, C.; Schölch, S. Prognostic Value of DLGAP5 in Colorectal Cancer. *Int. J. Colorectal Dis.* **2019**, *34* (8), 1455−1465.
(43) Fragoso, M. C. B. V.; Almeida, M. Q.; Mazzuco, T. L.; Mariani, B. M. P.; Brito, L. P.; Gonçalves, T. C.; Alencar, G. A.; Lima, L. de O.; Faria, A. M.; Bourdeau, I.; Lucon, A. M.; Freire, D. S.; Latronico, A. C.; Mendonca, B. B.; Lacroix, A.; Lerario, A. M. Combined Expression of BUB1B, DLGAP5, and PINK1 as Predictors of Poor Outcome in Adrenocortical Tumors: Validation in a Brazilian Cohort of Adult and Pediatric Patients. *Eur. J. Endocrinol.* **2012**, *166* (1), 61−67.
(44) Li, K.; Fu, X.; Wu, P.; Zhaxi, B.; Luo, H.; Li, Q. DLG7/DLGAP5 as a Potential Therapeutic Target in Gastric Cancer. *Chin. Med. J.* **2022**, *135* (13), 1616−1618.
(45) Shi, Y.-X.; Yin, J.-Y.; Shen, Y.; Zhang, W.; Zhou, H.-H.; Liu, Z.-Q. Genome-Scale Analysis Identifies NEK2, DLGAP5 and ECT2 as Promising Diagnostic and Prognostic Biomarkers in Human Lung Cancer. *Sci. Rep.* **2017**, *7* (1), No. 8072.
(46) Wang, Q.; Chen, Y.; Feng, H.; Zhang, B.; Wang, H. Prognostic and Predictive Value of HURP in Non-small Cell Lung Cancer. *Oncol. Rep.* **2018**, *39* (4), 1682−1692.
(47) Yamamoto, S.; Takayama, K.-I.; Obinata, D.; Fujiwara, K.; Ashikari, D.; Takahashi, S.; Inoue, S. Identification of New Octamer Transcription Factor 1-Target Genes Upregulated in Castration-Resistant Prostate Cancer. *Cancer Sci.* **2019**, *110* (11), 3476−3485.
(48) Weng, Y.; Liang, W.; Ji, Y.; Li, Z.; Jia, R.; Liang, Y.; Ning, P.; Xu, Y. Key Genes and Prognostic Analysis in HER2 + Breast Cancer. *Technol. Cancer Res. Treat.* **2021**, *20*, No. 1533033820983298.
(49) Matson, D. R.; Denu, R. A.; Zasadil, L. M.; Burkard, M. E.; Weaver, B. A.; Flynn, C.; Stukenberg, P. T. High Nuclear TPX2 Expression Correlates with TP53 Mutation and Poor Clinical Behavior in a Large Breast Cancer Cohort, but Is Not an Independent Predictor of Chromosomal Instability. *BMC Cancer* **2021**, *21* (1), 186.
(50) Zhang, X.; Pan, Y.; Fu, H.; Zhang, J. Nucleolar and Spindle Associated Protein 1 (NUSAP1) Inhibits Cell Proliferation and Enhances Susceptibility to Epirubicin In Invasive Breast Cancer Cells by Regulating Cyclin D Kinase (CDK1) and DLGAP5 Expression. *Med. Sci. Monit.* **2018**, *24*, 8553−8564.
(51) Qiu, J.; Xu, L.; Zeng, X.; Wu, Z.; Wang, Y.; Wang, Y.; Yang, J.; Wu, H.; Xie, Y.; Liang, F.; Lv, Q.; Du, Z. NUSAP1 Promotes the Metastasis of Breast Cancer Cells via the AMPK/PPARγ Signaling Pathway. *Ann. Transl. Med.* **2021**, *9* (22), 1689.
(52) Wu, S.; Su, R.; Jia, H. Cyclin B2 (CCNB2) Stimulates the Proliferation of Triple-Negative Breast Cancer (TNBC) Cells *In Vitro* and *In Vivo*. *Dis. Markers* **2021**, *2021*, No. 5511041.
(53) Lu, Z.-N.; Song, J.; Sun, T.-H.; Sun, G. UBE2C Affects Breast Cancer Proliferation through the AKT/mTOR Signaling Pathway. *Chin. Med. J.* **2021**, *134* (20), 2465−2474.
(54) Dastsooz, H.; Cereda, M.; Donna, D.; Oliviero, S. A Comprehensive Bioinformatics Analysis of UBE2C in Cancers. *Int. J. Mol. Sci.* **2019**, *20* (9), 2228.
(55) Oshi, M.; Gandhi, S.; Huyser, M. R.; Tokumaru, Y.; Yan, L.; Yamada, A.; Matsuyama, R.; Endo, I.; Takabe, K. MELK Expression in Breast Cancer Is Associated with Infiltration of Immune Cell and Pathological Compete Response (pCR) after Neoadjuvant Chemotherapy. *Am. J. Cancer Res.* **2021**, *11* (9), 4421−4437.
(56) Deng, J.-L.; Xu, Y.-H.; Wang, G. Identification of Potential Crucial Genes and Key Pathways in Breast Cancer Using Bioinformatic Analysis. *Front. Genet.* **2019**, *10*, 695.
(57) Zhu, L.; Zhang, Y.-J.; Wang, B.; Yang, L.; Zheng, Y.-Q.; Sun, L.-D.; Tian, L.; Chen, T.; Wang, J.-D. PCDHB17P/miR-145−3p/MELK/NF-κB Feedback Loop Promotes Metastasis and Angiogenesis of Breast Cancer. *Front. Oncol.* **2021**, *11*, No. 660307.
(58) Li, T.-F.; Zeng, H.-J.; Shan, Z.; Ye, R.-Y.; Cheang, T.-Y.; Zhang, Y.-J.; Lu, S.-H.; Zhang, Q.; Shao, N.; Lin, Y. Overexpression of Kinesin Superfamily Members as Prognostic Biomarkers of Breast Cancer. *Cancer Cell Int.* **2020**, *20*, 123.
(59) Cai, Y.; Mei, J.; Xiao, Z.; Xu, B.; Jiang, X.; Zhang, Y.; Zhu, Y. Identification of Five Hub Genes as Monitoring Biomarkers for Breast Cancer Metastasis in Silico. *Hereditas* **2019**, *156*, 20.
(60) Fang, L.; Liu, Q.; Cui, H.; Zheng, Y.; Wu, C. Bioinformatics Analysis Highlight Differentially Expressed CCNB1 and PLK1 Genes as Potential Anti-Breast Cancer Drug Targets and Prognostic Markers. *Genes* **2022**, *13* (4), No. 654.
(61) Yuan, F.; Wang, W. MicroRNA-802 Suppresses Breast Cancer Proliferation through Downregulation of FoxM1. *Mol. Med. Rep.* **2015**, *12* (3), 4647−4651.
(62) Zhao, X. miR-1258 Regulates Cell Proliferation and Cell Cycle to Inhibit the Progression of Breast Cancer by Targeting E2F1. *BioMed Res. Int.* **2020**, *2020*, No. 1480819.
(63) Wu, D.; Huo, C.; Jiang, S.; Huang, Y.; Fang, X.; Liu, J.; Yang, M.; Ren, J.; Xu, B.; Liu, Y. Exostosin1 as a Novel Prognostic and Predictive Biomarker for Squamous Cell Lung Carcinoma: A Study Based on Bioinformatics Analysis. *Cancer Med.* **2021**, *10* (8), 2787−2801.
(64) Bai, J.; Xu, J.; Zhao, J.; Zhang, R. lncRNA SNHG1 Cooperated with miR-497/miR-195−5p to Modify Epithelial-Mesenchymal

https://doi.org/10.1021/acsomega.4c00011
ACS Omega 2024, 9, 24379−24395

Transition Underlying Colorectal Cancer Exacerbation. *J. Cell. Physiol.* **2020**, *235* (2), 1453−1468.
(65) Chai, L.; Kang, X.-J.; Sun, Z.-Z.; Zeng, M.-F.; Yu, S.-R.; Ding, Y.; Liang, J.-Q.; Li, T.-T.; Zhao, J. MiR-497−5p, miR-195−5p and miR-455−3p Function as Tumor Suppressors by Targeting hTERT in Melanoma A375 Cells. *Cancer Manage. Res.* **2018**, *10*, 989−1003.
(66) Chen, S.; Wang, L.; Yao, X.; Chen, H.; Xu, C.; Tong, L.; Shah, A.; Huang, T.; Chen, G.; Chen, J.; Liu, T.-L.; Li, X.-T.; Zheng, J.-H.; Li, L. miR-195−5p Is Critical in REGγ-Mediated Regulation of Wnt/β-Catenin Pathway in Renal Cell Carcinoma. *Oncotarget* **2017**, *8* (38), 63986−64000.
(67) Luo, Q.; Zhang, Z.; Dai, Z.; Basnet, S.; Li, S.; Xu, B.; Ge, H. Tumor-Suppressive microRNA-195−5p Regulates Cell Growth and Inhibits Cell Cycle by Targeting Cyclin Dependent Kinase 8 in Colon Cancer. *Am. J. Transl Res.* **2016**, *8* (5), 2088−2096.
(68) Zhao, D.-L.; Wu, Q.-L. Effect of Inhibition to Yes-Related Proteins-Mediated Wnt/β-Catenin Signaling Pathway through miR-195−5p on Apoptosis of Gastric Cancer Cells. *Eur. Rev. Med. Pharmacol. Sci.* **2019**, *23* (15), 6486−6496.
(69) Zhou, W.-Y.; Zhang, M.-M.; Liu, C.; Kang, Y.; Wang, J.-O.; Yang, X.-H. Long Noncoding RNA LINC00473 Drives the Progression of Pancreatic Cancer via Upregulating Programmed Death-Ligand 1 by Sponging microRNA-195−5p. *J. Cell. Physiol.* **2019**, *234* (12), 23176−23189.
(70) Yan, L.-R.; Wang, A.; Lv, Z.; Yuan, Y.; Xu, Q. Mitochondria-Related Core Genes and TF-miRNA-Hub mrDEGs Network in Breast Cancer. *Biosci. Rep.* **2021**, *41* (1), No. BSR20203481.
(71) Yao, W.; Jia, X.; Xu, L.; Li, S.; Wei, L. MicroRNA-2053 Involves in the Progression of Esophageal Cancer by Targeting KIF3C. *Cell Cycle* **2021**, *20* (12), 1163−1172.
(72) Matboli, M.; Shafei, A. E.; Ali, M. A.; Gaber, A. I.; Galal, A.; Tarek, O.; Marei, M.; Khairy, E.; El-Khazragy, N.; Anber, N.; Abdel-Rahman, O. Clinical Significance of Serum DRAM1 mRNA, ARSA mRNA, Hsa-miR-2053 and lncRNA-RP1−86D1.3 Axis Expression in Malignant Pleural Mesothelioma. *J. Cell. Biochem.* **2019**, *120* (3), 3203−3211.
(73) Zhang, Z.; Li, J.; Huang, Y.; Peng, W.; Qian, W.; Gu, J.; Wang, Q.; Hu, T.; Ji, D.; Ji, B.; Zhang, Y.; Wang, S.; Sun, Y. Upregulated miR-1258 Regulates Cell Cycle and Inhibits Cell Proliferation by Directly Targeting E2F8 in CRC. *Cell Proliferation* **2018**, *51* (6), No. e12505.
(74) Wu, S.; Lu, J.; Zhu, H.; Wu, F.; Mo, Y.; Xie, L.; Song, C.; Liu, L.; Xie, X.; Li, Y.; lin, H.; Tang, H. A Novel Axis of circKIF4A-miR-637-STAT3 Promotes Brain Metastasis in Triple-Negative Breast Cancer. *Cancer Lett.* **2024**, *581*, No. 216508.

https://doi.org/10.1021/acsomega.4c00011
ACS Omega 2024, 9, 24379−24395